nature medicine

Article

https://doi.org/10.1038/s41591-024-03105-4

Sustained aviremia despite anti-retroviral therapy non-adherence in male children after in utero HIV transmission

Received: 6 October 2023

Accepted: 3 June 2024

Published online: 6 June 2024

Check for updates

A list of authors and their affiliations appears at the end of the paper

After sporadic reports of post-treatment control of HIV in children who initiated combination anti-retroviral therapy (cART) early, we prospectively studied 284 very-early-cART-treated children from KwaZulu-Natal, South Africa, after vertical HIV transmission to assess control of viremia. Eighty-four percent of the children achieved aviremia on cART, but aviremia persisting to 36 or more months was observed in only 32%. We observed that male infants have lower baseline plasma viral loads ($P = 0.01$). Unexpectedly, a subset ($n = 5$) of males maintained aviremia despite unscheduled complete discontinuation of cART lasting 3–10 months ($n = 4$) or intermittent cART adherence during 17-month loss to follow-up ($n = 1$). We further observed, in vertically transmitted viruses, a negative correlation between type I interferon (IFN-I) resistance and viral replication capacity (VRC) ($P < 0.0001$) that was markedly stronger for males than for females ($r = -0.51$ versus $r = -0.07$ for IFN-α). Although viruses transmitted to male fetuses were more IFN-I sensitive and of higher VRC than those transmitted to females in the full cohort ($P < 0.0001$ and $P = 0.0003$, respectively), the viruses transmitted to the five males maintaining cART-free aviremia had significantly lower replication capacity ($P < 0.0001$). These data suggest that viremic control can occur in some infants with in utero–acquired HIV infection after early cART initiation and may be associated with innate immune sex differences.

Studies of adult post-treatment controllers, such as the VISCONTI[1] or CHAMP cohorts[2–4], suggest that early combination anti-retroviral therapy (cART) initiation, low levels of immune activation and effective natural killer (NK) cell-mediated immunity may be key features contributing to HIV cure or remission. By contrast, immune control of cART-naive adult HIV infection is associated with very rapid and high levels of immune activation after infection and an aggressive anti-viral immune response driven by HIV-specific $CD8^+$ T cell activity[5–7]. Although, from historical studies, virus-specific $CD8^+$ T cells in cART-naive children are relatively ineffective in the first 1–2 years of life[8,9], and untreated HIV disease progression is substantially more rapid in children than in adults[9,10], it is proposed that early-cART-treated children may have a higher potential to achieve cART-free remission than adults[7]. First, cART can be initiated very early in the course of pediatric infection. Second, the highly regulated, tolerogenic early-life immune response[11] reduces the numbers of activated $CD4^+$ T cells available for HIV infection. Third, in early life, and in contrast with adults, NK responses are more effective mediators of control of HIV infection than virus-specific $CD8^+$ T cells[12]. Finally, again contrasting with adult-to-adult transmission, the vertically transmitted virus typically has relatively low replication capacity[13]. This is associated with low levels of immune activation, low pro-viral DNA loads and slow progression in the recipient[14]. These factors, therefore, would tend to lower viral reservoir size and increase cure potential among children. Furthermore, the ability to study both mother and child at birth provides access to the transmitted 'founder' virus, a precious resource in

e-mail: philip.goulder@paediatrics.ox.ac.uk.

https://doi.org/10.1038/s41591-024-03105-4

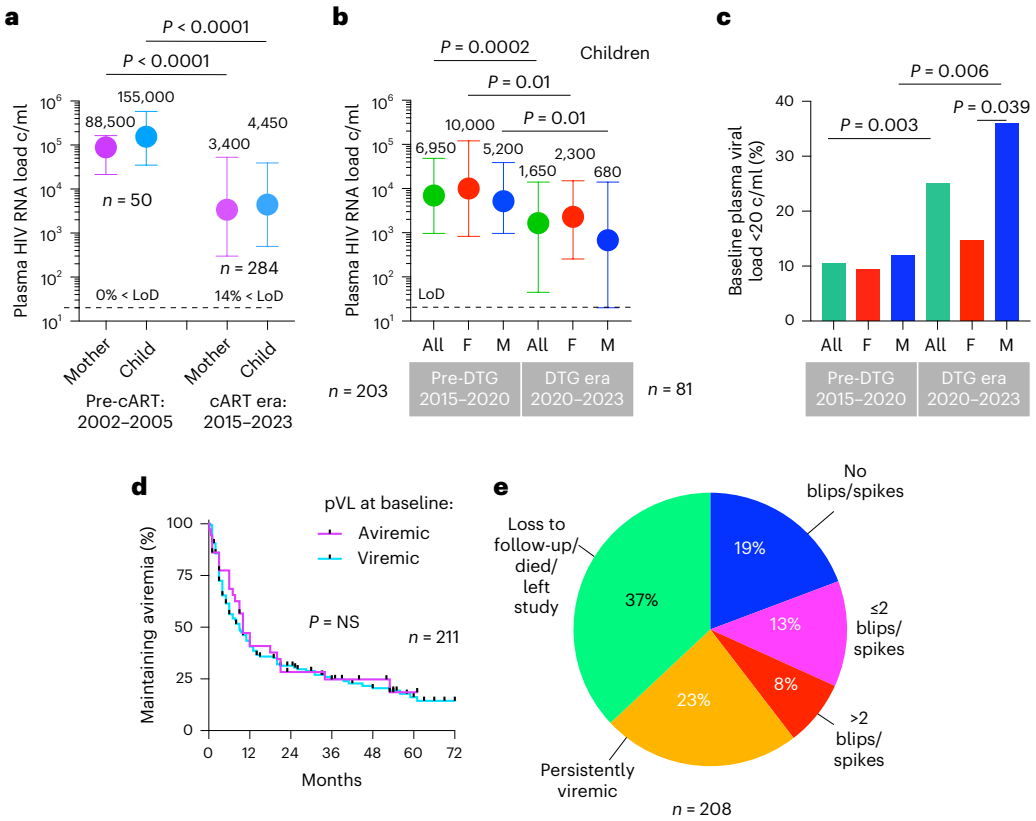

Fig. 1 | Impact of cART and changing cART regimens on baseline pVLs and maintenance of aviremia in pediatric HIV infection. a, pVLs at baseline in transmitting mothers and in utero–infected infants in the pre-cART era in KwaZulu-Natal, South Africa, 2002–2005, and in the cART era in KwaZulu-Natal, South Africa, 2015–2023. LoD, limit of detection: 20 HIV RNA copies per milliliter of plasma. Data are presented as median and IQR. **b**, Impact of DTG-based regimens on baseline pVLs in female and male in utero–infected infants. Data are presented as median and IQR. **c**, Impact of DTG-based regimens on the proportion of in utero–diagnosed infants with undetectable pVLs (<20 copies per milliliter). **d**, Time to viral rebound in study infants after suppression on cART: median 9 months in children aviremic at baseline (pVL <20 copies per milliliter) and 10 months in children viremic at baseline (pVL >20 copies per milliliter). The *P* value was determined using the log-rank Mantel–Cox test. **e**, Proportion of study cohort at 36 months after enrollment maintaining aviremia with or without viral blips/spikes; remaining on study but persistently viremic; or no longer on study as a result of loss to follow-up, death or relocation. The *P* values shown were determined using the two-sided Mann–Whitney *U*-test (**a**–**c**) and the log-rank Mantel–Cox test (**e**). c/ml, copies per milliliter; F, female; M, male.

understanding mechanisms of cART-free remission in those children who subsequently achieve it.

To identify which children, after early cART initiation, achieve undetectable HIV DNA loads and might, via additional immunotherapeutic interventions, ultimately achieve post-treatment control, we undertook an observational study between 2015 and 2023 of 284 mother–child pairs living with HIV (LWH) in KwaZulu-Natal, South Africa.

Results

Low baseline plasma HIV RNA loads in male infants

Diagnosis of in utero infection was made via detection of HIV nucleic acid from two or more separately drawn blood samples. Anti-retroviral therapy (ART) was started at birth in all children (AZT/NVP in 68% of cases, NVP alone in 32%), and cART (AZT/3TC/NVP) was initiated after confirmation of infection (median 1 day and 11 days of age, respectively, in children diagnosed via point-of-care (POC) ($n = 84$) and standard-of care (SOC) ($n = 200$) testing). However, in more than 90% of cases (262/284), cART was effectively initiated in children before birth via placental transfer of medications taken by antenatal mothers[15,16]. We, therefore, observed low baseline/birth plasma HIV RNA loads (pVLs) in children, especially since April 2020, when dolutegravir (DTG)-based cART regimens became first line in pregnancy (Fig. 1a–c). In males, baseline pVLs were 0.7 $\log_{10}$ lower than in females, after adjusting for cART regimen and age at enrolment ($P = 0.01$; Extended Data Table 1), consistent with previous studies showing lower pVL in males in the first 2 years of life[17,18], and 0.5 $\log_{10}$ lower total HIV DNA loads in male infants in this cohort, after adjusting for 25 other covariates[19]. However, maintenance of aviremia in children is generally short lived (Fig. 1d,e) because of challenges with cART adherence[20]. Thus, factors in addition to early cART initiation alone are required to achieve cART-free remission.

Five atypical cases maintaining cART-free aviremia

To better understand the relationship between pVL and cART adherence in the pediatric cohort, we analyzed plasma cART levels via liquid chromatography–tandem mass spectrometry (LC–MS/MS)[21], in relation to contemporaneous pVL. We determined the levels of all 13 ART drugs prescribed in South Africa but focused on lopinavir (LPV) because all children were treated with LPV/ritonavir (RTV) from 1 month of age, and its plasma level is directly related to anti-viral activity. Even allowing for natural variation in drug absorption, LPV levels lower than 500 ng ml^{-1} are considered strong evidence of non-adherence during the 24 h immediately before blood sampling (12-h trough levels[22,23] are typically 4,000–6,000 ng ml^{-1}). In a cross-sectional analysis of 94 individuals at 12 months of age, as expected, LPV levels higher than 500 ng ml^{-1} were strongly associated with aviremia ($P < 0.0001$; Fig. 2a). However, 26% ($n = 17$) of 65 aviremic individuals had low LPV levels. Analysis of subsequent timepoints (Extended Data Fig. 1) showed, in most of these children, either viral rebound within 12 months or sustained aviremia after cART resumption. The 25 children who were

https://doi.org/10.1038/s41591-024-03105-4

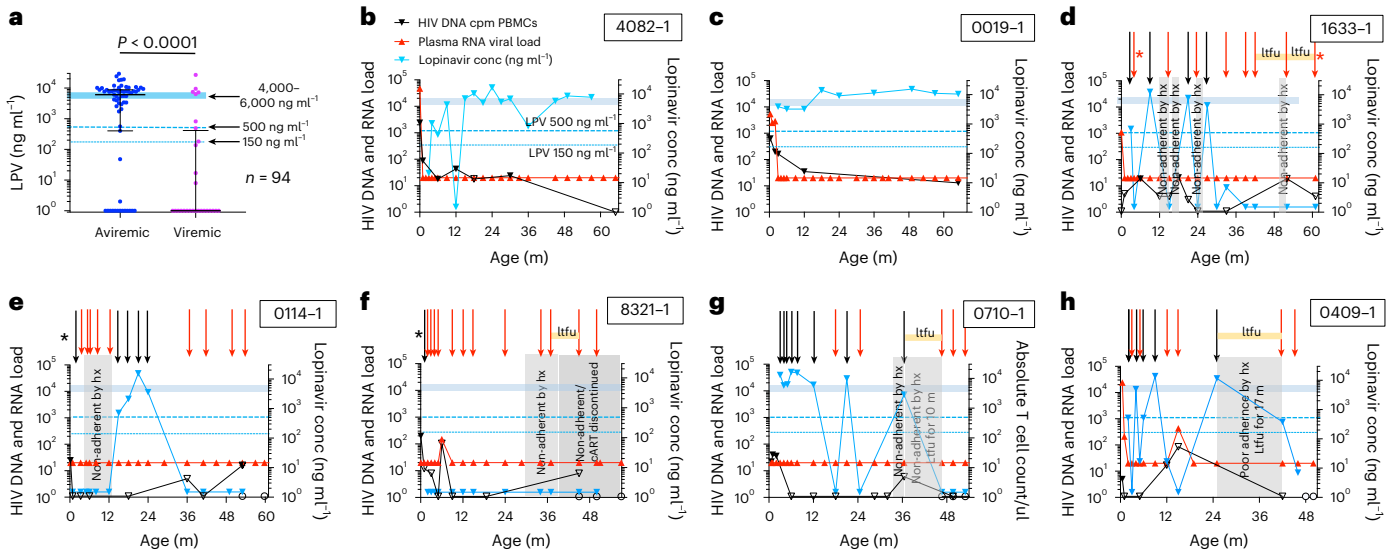

Fig. 2 | Maintenance of aviremia is dependent on cART adherence in most children and is independent of cART adherence in others. a, Cross-sectional analysis of 94 infants (median age 12 months) correlating pVLs with plasma concentrations of LPV. The normal range of LPV trough levels is 4,000–6,000 ng ml^{-1}; <150 ng ml^{-1} is below the level of quantification. The *P* value shown was determined using the two-sided Mann–Whitney *U*-test. **b**, Example of a child who was cART non-adherent temporarily at 12 months but maintained aviremia without viral rebound. **c**, Example of a child who maintained aviremia without viral rebound and without any evidence of cART non-adherence. **d**–**h**, Five 'atypical' children, 60-1633-1 (**d**), 80-0114-1 (**e**), 60-8321-1 (**f**), 70-0710-1 (**g**) and 80-0409-1 (**h**), maintaining aviremia and mostly undetectable or not significantly different from undetectable total DNA loads despite persistent cART non-adherence by history and by analysis of plasma cART levels. Periods of loss to follow-up are shown as 'ltfu'. Black arrows indicate timepoints at which LPV concentration was >500 ng ml^{-1}; red arrows indicate timepoints at which LPV concentration was <500 ng ml^{-1}; blue triangles indicate LPV concentration; red triangles indicate pVL copies per milliliter; solid black triangles indicate total HIV DNA load (cpm PBMCs) detected; open blank triangles indicate total HIV DNA load undetectable or not significantly different from undetectable; open circles indicate total HIV nucleic acid undetectable by GeneXpert; black asterisk indicates aviremia in association with prescribed cART that excluded LPV (that is, for 80-0114-1, AZT/3TC/NVP at 1 month of age); and red asterisks indicate cART non-adherent for the medications prescribed, but un-prescribed anti-retroviral drugs were detected at therapeutic levels at these timepoints, which could explain aviremia (see text for further specifics). conc, concentration; count/µl, count per microliter; m, months.

persistently aviremic to age ≥48 months, excluding the five atypical individuals discussed further below, were cART adherent at 90% of timepoints (Fig. 2b,c, Extended Data Fig. 1f and Extended Data Table 2).

Five children, however, differed considerably from these 25 age-matched 'typical' aviremic individuals in four key respects (Fig. 2d–h and Extended Data Table 2). First, according to history from the mother, in four cases, cART had been discontinued completely for 3–10 months, and, in the fifth case, cART adherence was intermittent for 17 months. Second, longitudinal analysis of plasma cART levels showed, after an initial period of adherence, that aviremia was subsequently maintained despite low/undetectable cART levels at most timepoints. Third, four of the five cases were temporarily lost to follow-up at the clinic for 8–17 months. In most cases in South Africa, monthly attendance at a specified clinic is the principal means of accessing the cART prescribed. Finally, despite strong evidence of cART non-adherence, in all five cases this was associated with sustained plasma aviremia, together with an undetectable total HIV DNA load at most timepoints, determined using a digital-droplet polymerase chain reaction (PCR) protocol. By contrast, total HIV DNA loads in the age-matched 'typical' aviremic children were, in most cases, detectable at all ages studied (at median age 46 months, median total HIV DNA load 14 copies per million (cpm) peripheral blood mononuclear cells (PBMCs), interquartile range (IQR) 5–74 cpm PBMCs; Supplementary Fig. 1). Moreover, to evaluate HIV-1 DNA further in the five 'atypical' individuals, single-genome PCR using different sets of primers previously shown to reliably amplify clade C proviral sequence[24–26] was attempted; however, we failed to detect any type of HIV-1 amplification products after analyzing 6–12 million PBMCs, isolated 48–61 months after birth, from each of these five infants (Extended Data Table 3).

Three children within this atypical group were breastfed, suggesting the possibility that maternal cART may have contributed to sustained aviremia in the children[16,27]. However, plasma efavirenz concentrations while breastfed were considerably below the therapeutic range[28] (1,000–4,000 ng ml^{-1}) and less than 5% of those in the maternal plasma (median 2,810 ng ml^{-1}; Extended Data Fig. 2).

A further possibility, that these five children may have been administered anti-HIV medications that they were not prescribed, was considered. In one child, 60-1633-1, at the 61-month timepoint, DTG, lamivudine and tenofovir prescribed to the mother were detected in the child's plasma; however, otherwise, maintenance of aviremia in these children was not explained by access to alternative cART.

Western blot analysis supports infection in atypical cases

The five children described here maintaining aviremia in the absence of cART more than met the criteria for HIV infection (Extended Data Table 4). Additionally, in four cases, HIV *gag* was amplified from baseline samples of plasma RNA, and mother–child sequences clustered on a phylogenetic tree (Extended Data Fig. 3, panel a). Furthermore, evidence of HIV infection in children arises from detection of antibody responses at ≥18 months of age[29,30]. Before this, anti-HIV antibody might represent maternal antibody crossing the placenta; breast milk–transferred maternal antibodies do not enter the neonatal or infant circulation in humans[31]. However, of 35 children (excluding the atypical cases) who maintained aviremia to ≥36 months without any viral blips or spikes recorded since achieving suppression of viremia by a median of 3 months, only four children tested western blot (WB) negative at 18 months, 24 months and 36 months (Extended Data Fig. 3b).

Similarly, of the five 'atypical' children who maintained aviremia despite cART non-adherence, none was WB negative at 18 months,

https://doi.org/10.1038/s41591-024-03105-4

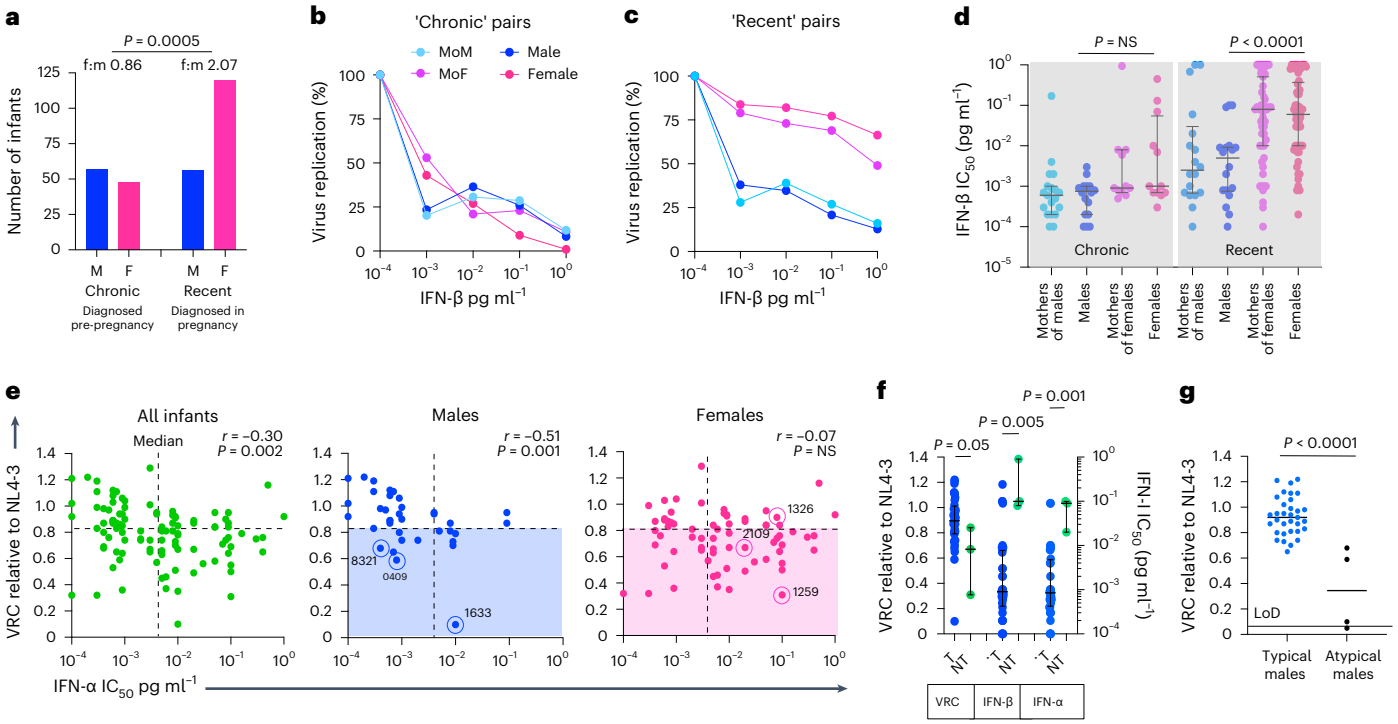

Fig. 3 | Viruses transmitted to female and male fetuses differ by VRC and IFN-I IC_{50}. **a**, Females are more susceptible to in utero transmission when mothers are recently infected but not when they are chronically infected. The *P* value shown was determined using a two-sided Fisher's exact test. **b**,**c**, Representative examples of viruses transmitted from chronically infected mothers to male and female fetuses (**b**) and from recently infected mothers to male and female fetuses (**c**). **d**, IFN-β IC_{50} values determined for 98 mother–child transmission pairs in the cohort. Data are presented as median and IQR. **e**, Relationship between VRC and IFN-α IC_{50} in viruses transmitted to males and to females. Blue open circles highlight males maintaining aviremia despite cART non-adherence. In the case of 80-0114-1, viral replication was detectable but at levels too low to measure VRC; therefore, IFN-I IC_{50} could not be determined for this child. Red open circles highlight viruses transmitted to the female twin but not to the male twin within three of five sex-discordant twinsets evaluated where, in each case, transmission occurred only in the female twin. Blue shading highlights viruses transmitted to males below the median VRC for all infants; red shading highlights viruses transmitted to females below the median VRC for all infants. The *r* values shown represent Spearman's rank correlation coefficient, and the *P* values shown were determined using the two-sided Student's *t*-test. **f**, Comparison of viruses transmitted to male singletons ($n = 36$) with those transmitted to female twins but not transmitted to male twins within three sex-discordant twinsets (that is, $n = 3$). Data are presented as median and IQR. VRC for 80-0114-1 was not included; including 80-0114-1, the *P* value becomes $P = 0.07$. T represents viruses transmitted to male fetuses; NT represents viruses not transmitted to male fetuses. **g**, VRC in 'typical' males (aviremia dependent on cART adherence) compared to the four 'atypical' males (aviremia not dependent on cART adherence) whose viruses were analyzed. This included VRC for 80-0114-1, which was detectable but too low to quantify. Excluding 80-0114-1, the *P* value becomes $P = 0.0006$. The *P* values shown in **d**, **f** and **g** were determined using the Mann–Whitney *U*-test (two-tailed). F, female; f:m, female to male; LoD, limit of detection; M, male.

24 months and 36 months (Extended Data Figs. 3 and 4). In four cases, there was increased WB reactivity across these timepoints. In the case of 70-0710-1, the absence of any WB bands at 18 months followed by the appearance of p24 and p55 Gag bands at 21 months coincided with cytomegalovirus infection, which strongly activates the immune system and lowers CD4/CD8 ratios[32] (Extended Data Fig. 4b).

Type I interferon–resistant, low viral replication capacity viruses are transmitted to females

Each of the five children described here maintaining aviremia in the absence of cART were male, contrasting with the cohort as a whole (60% female, $P = 0.01$, Fisher's exact test). We, therefore, considered possible mechanisms that might account for a higher rate of sustained cART-free aviremia in males. We previously reported[33] that female fetal susceptibility to in utero transmission is higher than that of male fetuses only in the setting of recently infected mothers. In this cohort, we found a female:male ratio of 2.07 in the setting of recently infected mothers and a female:male ratio of 0.86 in the setting of chronic maternal infection ($P = 0.0005$; Fig. 3a). In adult-to-adult transmission[34–36], the founder virus is highly type I interferon (IFN-I) resistant, but, over 6–12 months, the circulating viral quasi-species in the recipient become increasingly IFN-I sensitive. We, therefore, hypothesized, first, that fetuses born to chronically infected mothers are exposed in utero to IFN-I-sensitive viruses, whereas fetuses born to recently infected mothers are exposed principally to IFN-I-resistant viruses; and, second, that female fetuses would be more susceptible to IFN-I-resistant viruses because IFN-I production is higher in innate immune cells from female children, adolescents and adults than from males[37–40].

To determine the IFN-I sensitivity of transmitted viruses, we developed a high-throughput reporter assay using the IFN-I-sensitive U87 human glioblastoma cell line modified to express CXCR4 and CCR5 and stably transduced with a lentivirus vector to express secreted nanoluciferase in response to HIV-1 infection and Tat expression. We generated Gag-Pro-NL4-3 chimeric viruses from 98 mother–child pairs to determine IFN-α and IFN-β half-maximal inhibitory concentration (IC_{50}) values (Fig. 3b,c) and, at the same time, determine the viral replicative capacity (VRC) of transmitted viruses. As hypothesized, viruses transmitted to female fetuses were more IFN-I resistant than those transmitted to males but only in the setting of recent maternal infection ($P = 0.001$ and $P < 0.0001$ for IFN-α and IFN-β, respectively; Fig. 3d and Extended Data Fig. 5, panel a).

We next determined the VRC of the same Gag-Pro-NL4-3 viruses. The viruses transmitted to female fetuses overall had lower VRC than those transmitted to male fetuses ($P = 0.0003$; Extended Data Fig. 6).

https://doi.org/10.1038/s41591-024-03105-4

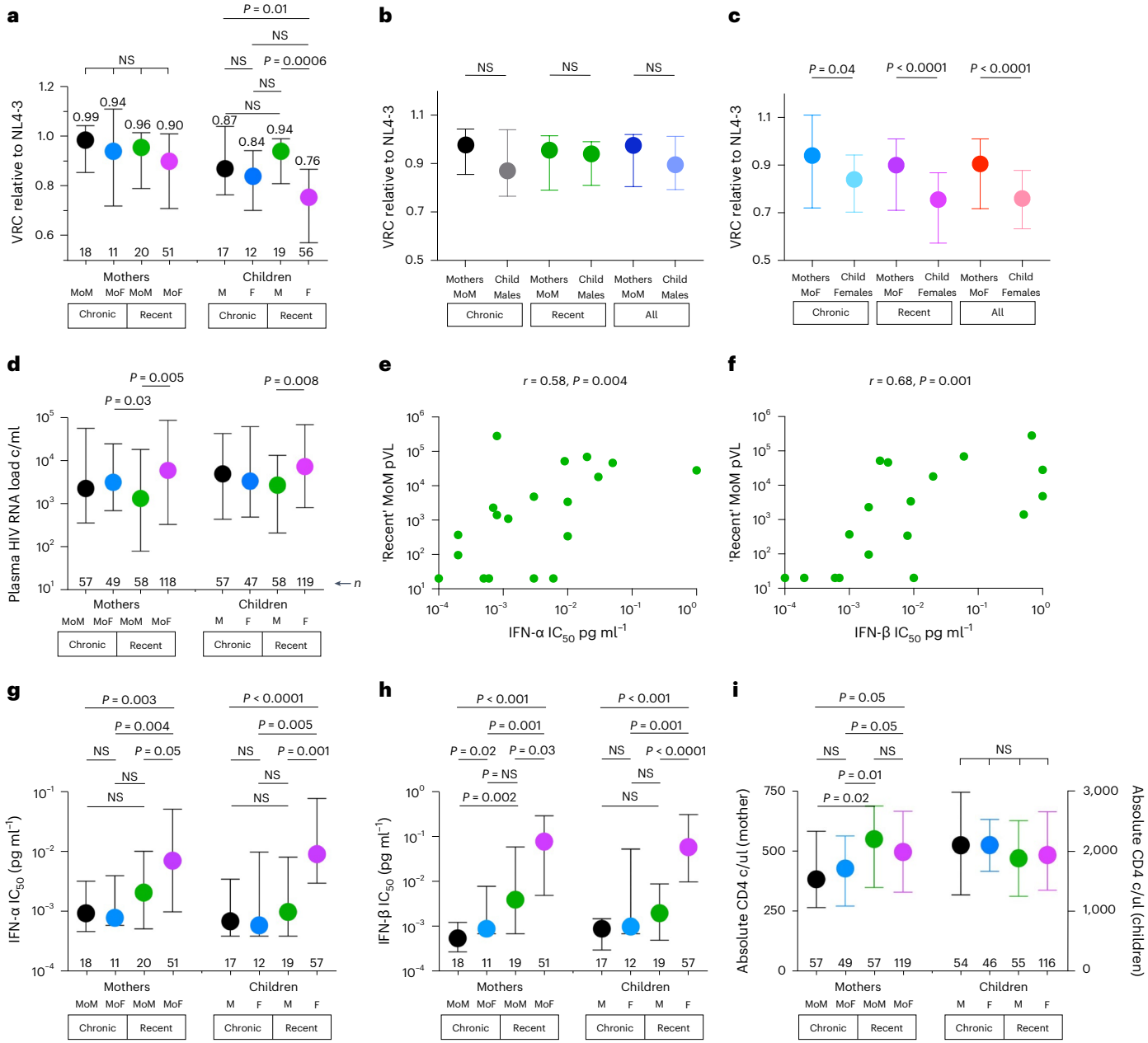

Fig. 4 | pVL, VRC, IFN-I IC_{50} values and absolute CD4 counts for the mother–child pairs within the Ucwaningo cohort. In **a**, **d** and **g**–**i**, mothers and infants are subdivided according to timing of maternal infection—chronically infected ('Chronic') and recently infected ('Recent')—and according to the sex of the infant: MoM, MoF, male (M) infants and female (F) infants. In all cases, data are from the time of enrollment/baseline. **a**, VRC relative to NL4-3. Median VRC values are shown. **b**,**c**, Comparison of VRC between MoM and males (**b**) and between MoF and females (**c**). **d**, pVLs. **e**,**f**, Correlation between pVL from recently infected MoM and IFN-I IC_{50} (IFN-α and IFN-β, **e** and **f**, respectively). *r* values shown are Spearman's rank correlation coefficients. *P* values shown were determined by the two-sided Student's *t*-test. **g**, IFN-α IC_{50}. **h**, IFN-β IC_{50}. **i**, Absolute CD4 counts. In **a**–**d** and **g**–**i**, data are presented as median and IQR. Other than for the tests applied in **e** and **f**, the *P* values shown in this figure were determined using two-tailed Mann–Whitney *U*-tests or, where comparisons were made between MoM and males or between MoF and females, using the two-tailed Wilcoxon matched-pairs signed-rank test. c/ml, copies per milliliter; c/ul, cells per microliter.

Viral mutations selected to confer IFN-I resistance may, like other immune escape variants[41–44], incur a cost to VRC and, hence, may be selected only in females where strong IFN-I innate immune responses impose sufficient selection pressure on the virus. Notably, we observed a negative correlation between IFN-I IC_{50} and VRC in the entire cohort (for IFN-α: infants, $r = -0.30$, $P = 0.002$, Fig. 3e; infants and mothers, $r = -0.27$, $P < 0.0001$, Extended Data Fig. 5b) and a stronger correlation among males than females (IFN-α: for males, $r = -0.51$, $P = 0.001$; for females, $r = -0.07$, *P* not significant (NS); Fig. 3e and Extended Data Fig. 5c).

To further characterize the differences between the viruses transmitted to female fetuses and not to male fetuses, we studied the five sex-discordant twinsets in the cohort in which transmission had arisen in only one twin. In our cohort, only the female twin acquired HIV in all five twinsets, similar to previously published twin studies[45]. Samples were available from three of the five twinsets. Compared to the transmitted viruses in male singletons, the three viruses transmitted to the female but not to the male twin (red-circled in Fig. 3e and Extended Data Fig. 5c) had somewhat lower VRCs ($P = 0.05$) but substantially

higher IFN-I IC_{50} values ($P = 0.001$ and $P = 0.005$ for IFN-α and IFN-β, respectively; Fig. 3f).

Lastly, in four of the five 'atypical' males described, the VRC of the viruses transmitted was substantially lower than that of the viruses transmitted to other males in the cohort (Fig. 3g; $P < 0.0001$ (in one instance, viral replication was detectable but at levels too low to quantify)). We propose that these collective findings are consistent with the hypothesis that in utero transmission followed by sustained productive infection in male infants is dependent upon the transmission of high-replication-capacity, IFN-I-sensitive viruses.

Selection of transmitted viruses by fetal immunity

To further investigate whether there is evidence of selection imposed by the fetal immune system, not only on whether transmission arises but also on the quality of viruses transmitted from the mother, we compared VRCs, IFN-α and IFN-β IC_{50} values, pVL, and absolute CD4 counts for the mothers of males (MoM), for the mothers of females (MoF), and for male and female infants, segregated by timing of maternal infection (Fig. 4). We observed that, although VRC ('fitness') does not differ between the viruses circulating in recently infected transmitting MoM and MoF (Fig. 4a), the viruses transmitted to female fetuses are of lower 'fitness' than those transmitted to male fetuses ($P = 0.0006$; Fig. 4a) and are also of substantially lower 'fitness' than those circulating in the MoF ($P < 0.0001$; Fig. 4c). By contrast, no difference was observed between the VRC/'fitness' of viruses circulating in MoM versus those transmitted to male fetuses (Fig. 4b).

Finally, we observed that pVL of recently infected MoM is lower than that of MoF (Fig. 4d). As expected, pVL in these mothers was strongly correlated with IFN-I IC_{50} ($r = 0.58$ and $r = 0.68$ for IFN-α and IFN-β, respectively; $P = 0.004$ and $P = 0.001$; Fig. 4b,c). Using a univariate linear regression model to determine the impact of IFN-α IC_{50} and IFNβ IC_{50} on pVL in the mothers (Supplementary Table 1), we note that the difference in IFN-I IC_{50} between transmitting MoM and transmitting MoF corresponds to a pVL difference of between 0.43 log_{10} and 0.78 log_{10} and that this, therefore, accounts fully for the observed 0.65 log_{10} difference in pVL between MoM and MoF.

Discussion

These observational studies of a cohort of 284 very-early-cART-treated children after in utero HIV infection identify a distinct group of five 'atypical' males maintaining aviremia in the absence of cART. Cases of post-treatment control after pediatric infection are rare[46–49] but have provided important evidence that functional cure or remission may be achievable in this setting. However, the conclusions that can be drawn from these and from the current study are limited by the small number of individuals described. Also, the cases previously described were quite dissimilar. In particular, the clade of virus, timing of vertical transmission and of cART initiation, age at viral suppression and CD4 nadir all differed from case to case. In the current study, the five atypical children are all male, whereas the cohort as a whole is 60% female. The four transmitted viruses analyzed had significantly lower VRC compared to those transmitted to 'typical' males. In two cases (60-1633-1 and 80-0114-1), VRC was exceptionally low. Of note, in both of these instances, the mothers seroconverted in the latter weeks of pregnancy, potentially increasing levels of immune activation in the fetus via the high levels of immune activation in the mother during acute infection. The risk of in utero vertical transmission in the absence of ART is increased three-fold by acute maternal infection[9]. These findings recall a report of spontaneous HIV clearance in a male infant after likely maternal seroconversion in pregnancy in the pre-cART era[50]. Together, these observations prompt the hypothesis that in utero transmission of high-replicative-capacity viruses may be needed to sustain HIV infection in males, whereas, in females, who have higher levels of immune activation both antenatally and postnatally[33,37], low-replicative-capacity/IFN-I-resistant viruses can propagate efficiently.

Previous studies in adults showed that the replication capacity of the transmitted virus influences pro-viral DNA load, levels of immune activation and disease outcome in the recipient[14]. Thus, the potential for cure/remission may initially be highest in those male infants who are infected with low-replicative-capacity viruses, especially if these are IFN-I sensitive and, therefore, more readily contained by innate immunity. However, beyond approximately 2 years of age, immune control of HIV is superior in females[17,18,51,52], and it is possible that the fine balance that exists between the disadvantages of a more activated immune system—in this case, greater susceptibility to in utero infection—and the advantages of more effective anti-viral immunity may favor females infected with low-replicative-capacity viruses in achieving post-treatment control later in childhood. Of note, the NK cell responses implicated in post-treatment control[1,4] and in reducing genome-intact HIV-1 DNA levels after ART initiation in neonates[24,53] have recently been shown to be stronger in female mice, despite lower absolute numbers of NK cells in females[54].

It is important to highlight limitations of this study. First, as mentioned above, the numbers of children described here achieving cART-free aviremia are small, and further studies are needed. Second, without a documented anti-retroviral therapy interruption (ATI), it is possible that cART was taken intermittently or that transient viral rebounds occurred between clinic visits and during periods of loss to follow-up. To that end, ATI studies were recently initiated in a selected subset of this cohort. To date, three of the five 'atypical' children described in this study have remained aviremic for more than 12 months during the ATI. In one case, 60-8321-1, cART has not been restarted so far for more than 30 months, after an additional period of 8 months of cART discontinuation in the child according to history. In adults, the median time to viral rebound after ATI is 3 weeks, 5% remaining suppressed 12 weeks after ATI[55–57]. ATI studies in children are rarer, with median time to viral rebound reportedly between 2 weeks and 8 weeks and 94–100% rebounding by 6 months[58–61]. Together, these data suggest that the five children reported here are highly unusual in maintaining aviremia for the duration of time described here.

A further caveat is the use of plasma cART testing to assess adherence, in conjunction with the history from the caregiver, pill counting and pharmacy records (Extended Data Table 2 and Supplementary Fig. 2). The measurement of cART levels in the plasma at clinic visit does not necessarily reflect cART adherence for the entire period of time between clinic visits. Nonetheless, even for a single sample taken at the 12-month timepoint, there is a strong correlation between cART levels and viremia. This is consistent with previous observations in this cohort that viral rebound is rarely explained by cART resistance and almost always by cART non-adherence[20]. Furthermore, these findings presented here indicate that aviremia in most children is highly cART adherence dependent.

An additional caveat is our use of Gag-Pro/NL4-3 chimeric viruses as opposed to full-length virus isolates to assess IFN-I sensitivity and VRC in this cohort. The reasons for using this approach are three-fold. First, the Gag-Pro/NL4-3 chimeric approach is high throughput, enabling the quasi-species of many individuals (98 mother–child pairs here) to be rapidly evaluated, allowing sex differences to be analyzed, which the substantially more labor-intensive approach using whole virus isolates precludes[34–36,62,63]. Second, our approach involves unbiased polyclonal amplification of the entire swarm of viruses present in the plasma sample, cloned into the NL4-3 backbone as a swarm of Gag-Pro/NL4-3 chimeric viruses. The chimeric virus swarm was shown in numerous studies[13,14,33,64–75] to be highly representative of the circulating quasi-species. The alternative, generating full-length viral isolates via single-genome amplification, is problematic because it is not at all certain whether each clone is representative of the viral swarm. Confirmation via deep sequencing of full-length virus is not generally feasible in the setting of low pVL levels that are fairly common in the children being studied here. Finally, although variation outside of Gag-Pro

including Env can also affect IFN-I sensitivity, the biological relevance of the Gag-Pro/NL4-3 virus has been thoroughly addressed[3,13,14,64–75]. The replication of these recombinant viruses is strongly correlated with that of full-length virus isolates and recapitulates clade-specific differences in replication[64]. Furthermore, the Gag-Pro region is known to bind to well-characterized IFN-I-stimulated restriction factors, such as TRIM5α and MX2 (refs. 76,77). Analysis of this relatively highly conserved part of the proteome in longitudinal studies of viruses harbored by individuals from acute into chronic infection should, in the future, facilitate the definition of specific variants that affect IFN-I sensitivity.

Next steps in evaluating the 'atypical' males described here would first include ATI studies to identify additional cases of very-early-cART-treated children who can maintain cART-free aviremia. To date, we have depended on chance findings of aviremia in children after prolonged cART discontinuation. However, the current study and reports from the P1115 trial[78] suggest that prospective ATI studies will reveal additional cases that, together, would facilitate identification of genetic, virological and immune factors contributing to post-treatment control in children. In addition, as these children progress to adolescence, it may become feasible to undertake, via leukapheresis, more comprehensive analyses of the viral reservoir.

In conclusion, irrespective of how early cART is initiated, maintenance of aviremia in children is highly cART dependent, and, in most cases, cure/remission strategies will depend on interventions additional to early cART initiation. However, a small subset of early-cART-treated children exists that may achieve post-treatment control. The factors identified in this cohort that associate with viral control include male sex and the transmission of low-replicative-capacity, IFN-I-sensitive virus. Most adult studies of ATI have focused on males from resource-rich settings, and initial indications are that differences may exist between the sexes with respect to post-treatment control in resource-limited settings[79]. Further studies are needed to determine the impact of sex and other genetic, viral and immune factors on post-treatment control at different ages as well as the additional interventions that will accelerate functional cure in early-cART-treated children and identify the subsets of children that are most likely to achieve it.

Online content

Any methods, additional references, Nature Portfolio reporting summaries, source data, extended data, supplementary information, acknowledgements, peer review information; details of author contributions and competing interests; and statements of data and code availability are available at https://doi.org/10.1038/s41591-024-03105-4.

References

1. Saez-Cirion, A. et al. Post-treatment HIV-1 controllers with a long-term virological remission after the interruption of early initiated antiretroviral therapy ANRS VISCONTI study. *PLoS Pathog.* **9**, e1003211 (2013).
2. Li, J. Z. et al. The size of the expressed HIV reservoir predicts timing of viral rebound after treatment interruption. *AIDS* **30**, 343–353 (2016).
3. Namazi, G. et al. The control of HIV after antiretroviral medication pause (CHAMP) study: post-treatment controllers identified from 14 clinical studies. *J. Infect. Dis.* **218**, 1954–1963 (2018).
4. Etemad, B. H. et al. HIV post-treatment controllers have distinct immunological and virological features. *Proc. Natl Acad. Sci. USA* **120**, e2218960120 (2023).
5. Ndhlovu, N. et al. Magnitude and kinetics of CD8$^+$ T-cell activation during hyper-acute HIV-1 infection impact viral setpoint. *Immunity* **43**, 591–604 (2015).
6. Pereyra, F. et al. Increased coronary atherosclerosis and immune activation in HIV-1 elite controllers. *AIDS* **26**, 2409–2412 (2012).
7. Goulder, P. & Deeks, S. HIV control: is getting there the same as staying there? *PLoS Pathog.* **14**, e1007222 (2018).
8. Leitman, E. M. et al. Role of HIV-specific CD8$^+$ T-cells in paediatric HIV cure strategies following widespread early viral escape. *J. Exp. Med.* **214**, 3239–3261 (2017).
9. Goulder, P. J. R., Lewin, S. R. & Leitman, E. M. Paediatric HIV infection: the potential for cure. *Nat. Rev. Immunol.* **16**, 259–271 (2016).
10. Newell, M. L. et al. Mortality of infected and uninfected infants born to HIV-infected mothers in Africa: a pooled analysis. *Lancet* **364**, 1236–1243 (2004).
11. Kollman, T. R. et al. Innate immune function by Toll-like receptors: distinct responses in newborns and the elderly. *Immunity* **37**, 771–778 (2012).
12. Vieira, V. A. et al. An HLA-I signature favouring KIR-educated natural killer cells mediates immune control of HIV in children and contrasts with the HLA-B-restricted CD8$^+$ T-cell mediated immune control in adults. *PLoS Pathog.* **17**, e1010090 (2021).
13. Naidoo, V. et al. Mother-to-child transmission bottleneck selects for consensus virus with low Gag-protease-driven replication capacity. *J. Virol.* **91**, e00518-17 (2017).
14. Claiborne, D. T. et al. Replicative fitness of transmitted HIV-1 drives acute immune activation, proviral load in memory CD4$^+$ T-cells and disease progression. *Proc. Natl Acad. Sci. USA* **112**, E1480–E1489 (2015).
15. Rimawi, B. H. et al. Pharmacokinetics and Placental Transfer of Elvitegravir, Dolutegravir, and Other Antiretrovirals during Pregnancy. *Antimicrob. Agents Chemother.* **61**, e02213-16 (2017).
16. Hodel, E. M., Marzolini, C., Waitt, C. & Rakhmanina, N. Pharmacokinetics, placental and breast milk transfer of antiretroviral drugs in pregnant and lactating women living with HIV. *Curr. Pharm. Des.* **25**, 556–576 (2019).
17. European Collaborative Study. Level and pattern of HIV-1-RNA viral load over age: differences between girls and boys? *AIDS* **16**, 97–104 (2002).
18. Ruel, T. et al. Sex differences in HIV RNA level and CD4 cell percentage during childhood. *Clin. Infect. Dis.* **53**, 592–599 (2011).
19. Millar, J. et al. Early initiation of antiretroviral therapy following in utero HIV infection is associated with low viral reservoirs but other factors determine viral rebound. *J. Infect. Dis.* **224**, 1925–1934 (2021).
20. Millar, J. R. et al. High-frequency failure of combination antiretroviral therapy in paediatric HIV infection is associated with unmet maternal needs causing maternal non-adherence. *EClinicalMedicine* **22**, 100344 (2020).
21. Koehn, J. & Ho, R. Novel liquid chromatography-tandem mass spectrometry method for simultaneous detection of anti-HIV drugs lopinavir, ritonavir, and tenofovir in plasma. *Antimicrob. Agents Chemother.* **58**, 2675–2680 (2014).
22. Best, B. M. et al. Pharmacokinetics of lopinavir/ritonavir crushed versus whole tablets in children. *J. Acquir. Immune Defic. Syndr.* **58**, 385–391 (2012).
23. Bouazza, N. et al. Lopinavir/ritonavir plus lamivudine and abacavir or zidovudine dose ratios for paediatric fixed-dose combinations. *Antivir. Ther.* **20**, 225–233 (2015).
24. Garcia-Broncano, P. et al. Early antiretroviral therapy in neonates with HIV-1 infection restricts viral reservoir size and induces a distinct innate immune profile. *Sci. Transl. Med.* **11**, eaax7350 (2019).
25. Lee, G. Q. et al. HIV-1 DNA sequence diversity and evolution during acute subtype C infection. *Nat. Commun.* **10**, 2737 (2019).
26. Koofhethile, C. K. et al. CD8$^+$ T cell breadth with and without protective HLA class I alleles. *J. Virol.* **90**, 6818–6831 (2016).
27. Shapiro, R. L. et al. Therapeutic levels of lopinavir in late pregnancy and abacavir passage into breast milk in the Mma Bana Study, Botswana. *Antivir. Ther.* **18**, 585–590 (2013).

28. Marzolini, C. et al. Efavirenz plasma levels can predict treatment failure and central nervous system side effects in HIV-1-infected patients. *AIDS* **15**, 11–75 (2001).
29. World Health Organization. *Recommendations on the Diagnosis of HIV Infection in Infants and Children* (World Health Organization, 2010); https://iris.who.int/bitstream/handle/10665/44275/9789241599085_eng.pdf?sequence=1
30. McManus, M. et al. Quantitative HIV-1 antibodies correlate with plasma HIV-1 viral RNA and cell-associated DNA levels in children on antiretroviral therapy. *Clin. Infect. Dis.* **68**, 1725–1732 (2019).
31. Van de Perre, P. Transfer of antibody via mother's milk. *Vaccine* **21**, 3374–3376 (2003).
32. Freeman, M. L., Mudd, J. C., Shive, C. L., Younes, S. A. & Panigrahi, S. CD8 T-cell expansion and inflammation linked to CMV coinfected in ART-treated HIV infection. *Clin. Infect. Dis.* **62**, 392–396 (2016).
33. Adland, E. et al. Sex-specific innate immune selection of HIV-1 in utero is associated with increased female susceptibility to infection. *Nat. Commun.* **11**, 1767 (2020).
34. Iyer, S. S. et al. Resistance to type 1 interferons is a major determinant of HIV-1 transmission fitness. *Proc. Natl Acad. Sci. USA* **114**, E590–E599 (2017).
35. Fenton-May, A. E. et al. Relative resistance of HIV-1 founder viruses to control by interferon-alpha. *Retrovirology* **10**, 146 (2013).
36. Gondim, M. et al. Heightened resistance to type 1 interferons characterizes HIV-1 at transmission and following treatment interruption. *Sci. Transl. Med.* **13**, eabd8179 (2021).
37. Meier, A. et al. Sex differences in the Toll-like receptor-mediated response of plasmacytoid dendritic cells to HIV-1. *Nat. Med.* **15**, 955–959 (2009).
38. Berghöfer, B. et al. TLR7 ligands induce higher IFN-α production in females. *J. Immunol.* **117**, 2088–2096 (2006).
39. Webb, K. et al. Sex and pubertal differences in the type 1 interferon pathway associate with both X chromosome number and serum sex hormone concentration. *Front. Immunol* **9**, 3167 (2019).
40. Sampson, O. et al. A simple, robust flow cytometry-based whole blood assay for investigating sex differential interferon alpha production by plasmacytoid dendritic cells. *J. Immunol. Methods* **504**, 113263 (2022).
41. Leslie, A. J. et al. HIV evolution: CTL escape mutation and reversion after transmission. *Nat. Med.* **10**, 282–289 (2004).
42. Martinez-Picado, J. et al. Fitness cost of escape mutation in p24 Gag in association with control of HIV-1. *J. Virol.* **80**, 3617–3623 (2006).
43. Schneidewind, A. et al. Structural and functional constraints limit options for CTL escape in the immunodominant HLA-B27 restricted epitope in HIV-1 capsid. *J. Virol.* **82**, 5594–5605 (2008).
44. Neumann-Haefelin, C. et al. HLA-B27 selects for rare escape mutations that significantly impair hepatitis C virus replication and require compensatory mutations. *Hepatology* **54**, 1157–1166 (2011).
45. Biggar, R. et al. Higher in utero and perinatal infection risk in girls than boys. *J. Acquir. Immune Defic. Syndr.* **41**, 509–513 (2006).
46. Persaud, D. et al. Absence of detectable HIV-1 viremia after treatment cessation in an infant. *N. Engl. J. Med.* **369**, 1828–1835 (2013).
47. Luzuriaga, K. et al. Viraemic relapse after HIV-1 remission in a perinatally infected child. *N. Engl. J. Med.* **372**, 786–788 (2015).
48. Frange, P. et al. HIV-1 virological remission lasting more than 12 years after interruption of early antiretroviral therapy in a perinatally infected teenager enrolled in the French ANRS EPF-CO10 paediatric cohort: a case report. *Lancet HIV* **3**, e49–e54 (2016).
49. Violari, A. et al. A child with perinatal infection and long-term sustained virological control following anti-retroviral treatment cessation. *Nat. Commun.* **10**, 412 (2019).
50. Bryson, Y. et al. Clearance of HIV infection in a perinatally infected infant. *N. Eng. J. Med* **332**, 833–838 (1995).
51. Gandhi, M. et al. Does patient sex affect human immunodeficiency virus levels? *Clin. Infect. Dis.* **35**, 313–322 (2002).
52. Yang, O. O. et al. Demographics and natural history of HIV-1-infected spontaneous controllers of viraemia. *AIDS* **31**, 1091–1098 (2017).
53. Hartana, C. A. et al. Immune correlates of HIV-1 reservoir cell decline in early-treated infants. *Cell Rep.* **40**, 111126 (2022).
54. Cheng, M. I. et al. The X-linked epigenetic regulator UTX controls NK cell-intrinsic sex differences. *Nat. Immunol.* **24**, 780–791 (2023).
55. Li, J. Z. et al. Time to viral rebound after interruption of modern antiretroviral therapies. *Clin. Infect. Dis.* **74**, 865–870 (2022).
56. Zhou, C. et al. Factors associated with post-treatment control of viral load in HIV-infected patients: a systematic review and meta-analysis. *Int. J. Infect. Dis.* **129**, 216–227 (2023).
57. Colby, D. J. et al. Rapid HIV RNA rebound after antiretroviral treatment interruption in persons durably suppressed in Fiebig I acute HIV infection. *Nat. Med.* **24**, 923–926 (2018).
58. Paediatric European Network for Treatment of AIDS. Response to planned treatment interruptions in HIV infection varies across childhood. *AIDS* **24**, 231–241 (2010).
59. Vieira, V. A. et al. Slow progression of pediatric HIV associates with early $CD8^+$ T cell PD-1 expression and a stem-like phenotype. *JCI Insight* **8**, e156049 (2023).
60. Shapiro, R. L. et al. Broadly neutralizing antibody treatment maintained HIV suppression in children with favorable reservoir characteristics in Botswana. *Sci. Transl. Med.* **15**, eadh0004 (2023).
61. Violari, A. et al. *Proc. 25th Conference on Retroviruses and Opportunistic Infections* (International Antiviral Society–USA, 2018); https://penta-id.org/publications/time-to-viral-rebound-after-stopping-art-in-children-treated-from-infancy-in-cher/
62. Parrish, N. F. et al. Phenotypic properties of transmitted founder HIV-1. *Proc. Natl Acad. Sci. USA* **110**, 6626–6633 (2013).
63. Deymier, M. J. et al. Heterosexual transmission of subtype C HIV-1 selects consensus-like variants without increased replication capacity or IFN-α resistance. *PLoS Pathog.* **11**, e1005154 (2015).
64. Kiguoya, M. W. et al. Subtype-specific differences in Gag-Pro-driven replication capacity are consistent with intersubtype differences in HIV-1 disease progression. *J. Virol.* **91**, e00253-17 (2017).
65. Miura, T. et al. HLA-associated alterations in replication capacity of chimeric NL4-3 viruses carrying *gag-protease* from elite controllers of human immunodeficiency virus type 1. *J. Virol.* **83**, 140–149 (2009).
66. Miura, T. et al. HLA-B57/B*5801 human immunodeficiency virus type 1 elite controllers select for rare Gag variants associated with reduced viral replication capacity and strong cytotoxic T-lymphocyte recognition. *J. Virol.* **83**, 2743–2755 (2009).
67. Prado, J. G. et al. Replicative capacity of human immunodeficiency virus type 1 transmitted from mother to child is associated with pediatric disease progression rate. *J. Virol.* **84**, 492–502 (2010).
68. Brockman, M. et al. Early selection in Gag by protective HLA alleles contributes to reduced HIV-1 replication capacity that may be largely compensated for in chronic infection. *J. Virol.* **84**, 11937–11949 (2010).

69. Wright, J. et al. Gag-protease-mediated replication capacity in HIV-1 clade C chronic infection: associations with HLAS type and clinical parameters. *J. Virol.* **84**, 10820–10831 (2010).
70. Huang, K. H. et al. Progression to AIDS in South Africa is associated with both reverting and compensatory viral mutations. *PLoS ONE* **6**, e19018 (2011).
71. Boutwell, C. et al. Frequent and variable CTL escape-associated fitness costs in the HIV-1 Gag proteins. *J. Virol.* **87**, 3952–3965 (2013).
72. Nomura, S. et al. Significant reductions in Gag-Protease-mediated HIV-12 replication capacity during the course of the epidemic in Japan. *J. Virol.* **87**, 1465–1476 (2013).
73. Juarez-Molina, C. et al. Impact of HLA selection pressure on HIV fitness at a population level in Mexico and Barbados. *J. Virol.* **88**, 10392–10398 (2014).
74. Payne, R. et al. Impact of HLA-driven HIV adaptation on virulence in populations of high HIV seroprevalence. *Proc. Natl Acad. Sci. USA* **111**, E5393–E5400 (2014).
75. Adland, E. et al. Discordant impact of HLA on viral replicative capacity and disease progression in pediatric and adult HIV infection. *PLoS Pathog.* **11**, e1004954 (2015).
76. Doyle, T. et al. HIV-1 and interferons: who's interfering with whom? *Nat. Rev. Microbiol.* **13**, 403–413 (2015).
77. Jimenez-Guardeno, J. M. et al. Immunoproteasome activation enables human TRIM5α restriction of HIV-1. *Nat. Microbiol.* **4**, 933–940 (2019).
78. Persaud, D. et al. *Proc. 2024 Conference on Retroviruses and Opportunistic Infections* (International Antiviral Society–USA, 2024); https://www.croiconference.org/abstract/art-free-hiv-1-remission-in-very-early-treated-children-results-from-impaact-p1115/
79. Le, C. N. et al. Time to viral rebound and safety after antiretroviral treatment interruption in postpartum women compared to men. *AIDS* **33**, 2149–2156 (2019).

Nomonde Bengu[1,2,26], Gabriela Cromhout[2,3,26], Emily Adland[4,26], Katya Govender[5], Nicholas Herbert[4], Nicholas Lim[4], Rowena Fillis[6], Kenneth Sprenger[2], Vinicius Vieira[4], Samantha Kannie[7], Jeroen van Lobenstein[7], Kogielambal Chinniah[8], Constant Kapongo[1], Roopesh Bhoola[6], Malini Krishna[6], Noxolo Mchunu[2], Giuseppe Rubens Pascucci[9,10], Nicola Cotugno[9,11], Paolo Palma[9,11], Alfredo Tagarro[12,13,14], Pablo Rojo[12], Julia Roider[15], Maria C. Garcia-Guerrero[16], Christina Ochsenbauer[17], Andreas Groll[18], Kavidha Reddy[5], Carlo Giaquinto[19], Paolo Rossi[9,11], Seohyun Hong[20], Krista Dong[20], M. Azim Ansari[21], Maria C. Puertas[16,22], Thumbi Ndung'u[2,5,20,23], Edmund Capparelli[24], Mathias Lichterfeld[20], Javier Martinez-Picado[16,22], John C. Kappes[17,25], Moherndran Archary[3] & Philip Goulder[2,4,5,20] ✉

[1]Queen Nandi Regional Hospital, Empangeni, South Africa. [2]HIV Pathogenesis Programme, Doris Duke Medical Research Institute, Nelson R. Mandela School of Medicine, University of KwaZulu-Natal, Durban, South Africa. [3]Department of Paediatrics, University of KwaZulu-Natal, Durban, South Africa. [4]Department of Paediatrics, University of Oxford, Oxford, UK. [5]Africa Health Research Institute, Durban, South Africa. [6]Harry Gwala Regional Hospital, Pietermaritzburg, South Africa. [7]General Justice Gizenga Mpanza Regional Hospital, Stanger, South Africa. [8]Mahatma Gandhi Memorial Hospital, Durban, South Africa. [9]Clinical Immunology and Vaccinology Unit, IRCCS, Ospedale Pediatrico Bambino Gesù, Rome, Italy. [10]Probiomics S.r.l., Rome, Italy. [11]University of Rome Tor Vergata, Rome, Italy. [12]Fundación de Investigación Biomédica Hospital 12 de Octubre, Instituto de Investigación 12 de Octubre (imas12), Madrid, Spain. [13]Department of Pediatrics, Infanta Sofia University Hospital and Henares University Hospital Foundation for Biomedical Research and Innovation, Madrid, Spain. [14]Universidad Europea de Madrid, Madrid, Spain. [15]LMU University Hospital, Munich, Germany. [16]IrsiCaixa AIDS Research Institute, Barcelona, Spain. [17]University of Alabama at Birmingham, Birmingham, AL, USA. [18]TU Dortmund University, Dortmund, Germany. [19]University of Padova, Padua, Italy. [20]Ragon Institute of MGH, MIT and Harvard, Boston, MA, USA. [21]Nuffield Department of Medicine, University of Oxford, Oxford, UK. [22]Consorcio Centro de Investigación Biomédica en Red de Enfermedades Infecciosas (CIBERINFEC), Instituto de Salud Carlos III, Madrid, Spain. [23]Division of Infection and Immunity, University College London, London, UK. [24]University of California San Diego, San Diego, CA, USA. [25]Birmingham Veterans Affairs Medical Center, Research Service, Birmingham, AL, USA. [26]These authors contributed equally: Nomonde Bengu, Gabriela Cromhout, Emily Adland. ✉e-mail: philip.goulder@paediatrics.ox.ac.uk

Methods

Study participants

The Ucwaningo Lwabantwana (meaning 'Learning from Children') is a cohort of 284 in utero–infected children enrolled and followed in KwaZulu-Natal, South Africa, from 2015 to 2023. All infants were tested at birth via the SoC dried blood spot total nucleic acid PCR (COBAS AmpliPrep/COBAS TaqMan HIV-1 Qualitative PCR v2, Roche Molecular Diagnostics) that was run in a central laboratory. If the result of this test was positive or indeterminate, a confirmatory or repeat test, respectively, was undertaken at approximately 7 days of age. All children born to mothers LWH received ART in the delivery room within minutes of birth (either NVP alone or AZT plus NVP, according to local guidelines). Infants of mothers at high risk of in utero HIV transmission were also tested for HIV-1 as soon as possible after birth using PoC testing (in addition to the SoC testing) to detect total nucleic acid via PCR on whole blood (GeneXpert Qualitative HIV-1 PCR, Cepheid): 84 infants in the cohort were diagnosed via PoC testing, and the remaining 200 were diagnosed via SoC testing. In all 284 enrollees, confirmed diagnosis required two separate samples detecting HIV nucleic acid. Baseline data were collected at a median of 1.0 (IQR 0.9–1.8) day of age and 11 (IQR 9–14) days of age from the PoC-diagnosed and SoC-diagnosed infants, respectively. Initial cART for infants with confirmed HIV infection comprised twice-daily NVP, AZT and lamivudine (3TC) as per local guidelines. This regimen was switched to RTV-boosted LPV, 3TC and abacavir (ABC) at 42 weeks corrected gestational age or at 1 month of age. Mother and infant follow-up occurred monthly for 6 months and then every 3 months. At each visit, blood was drawn for $CD4^+$ T cell quantification, pVL (HIV-1 RNA PCR, NucliSens) and storage of PBMCs and plasma. This study was approved by the Biomedical Research Ethics Committee of the University of KwaZulu-Natal and the Oxfordshire Research Ethics Committee. Written informed consent for the infant's and mother's participation in the study was obtained from the mother or the infant's legal guardian.

Viral RNA isolation and nested RT–PCR amplification of *gag-protease* from plasma

Viral RNA was isolated from plasma by use of a QIAamp Viral RNA Mini Kit (Qiagen). The *Gag-Protease* region was amplified by PCR with reverse transcription (RT–PCR) from plasma HIV-1 RNA using a SuperScript III One-Step Reverse Transcriptase Kit (Invitrogen) and the following *Gag-protease*-specific primers: 2cRx, 5′ CAC TGC TTA AGC CTC AAT AAA GCT TGC C 3′ (HXB2 nucleotides 512–539), and 623Fi, 5′ TTT AAC CCT GCT GGG TGT GGT ATT CCT 3′ (nucleotides 2,851–2,825). Second-round PCR was performed using 100-mer primers that completely matched the pNL4-3 sequence using Takara EX Taq DNA Polymerase, Hot Start version (Takara Bio). One hundred microliters of reaction mixture was composed of 10 µl of 10× EX Taq Buffer, 4 µl of deoxynucleoside triphosphate mix (2.5 mM each), 6 µl of 10 µM forward primer, *Gag-Pro* F (GAC TCG GCT TGC TGA AGC GCG CAC GGC AAG AGG CGA GGG GCG GCG ACT GGT GAG TAC GCC AAA AAT TTT GAC TAG CGG AGG CTA GAA GGA GAG AGA TGG G, 695–794) and reverse primer, *Gag-Pro* R (GGC CCA ATT TTT GAA ATT TTT CCT TCC TTT TCC ATT TCT GTA CAA ATT TCT ACT AAT GCT TTT ATT TTT TCT TCT GTC AAT GGC CAT TGT TTA ACT TTT G, 2,646–2,547), 0.5 µl of enzyme and 2 µl of first-round PCR product and DNase-RNase-free water. Thermal cycler conditions were as follows: 94 °C for 2 min followed by 40 cycles of 94 °C for 30 s, 60 °C for 30 s and 72 °C for 2 min and then followed by 7 min at 72 °C. PCR products were purified using a QIAquick PCR Purification Kit (Qiagen) according to the manufacturer's instructions.

Generation of recombinant *Gag-Protease* viruses

A deleted version of pNL4-3 was constructed that lacks the entire *Gag* and *Protease* region (Stratagene QuikChange XL kit), replacing this region with a BstE II (New England Biolabs) restriction site at the 5′ end of *Gag* and at the 3′ end of *protease*. To generate recombinant viruses, 10 µg of BstEII-linearized plasmid plus 50 µl of the second-round amplicon (approximately 2.5 µg) were mixed with 2×10^6 cells of a Tat-driven green fluorescent protein (GFP) reporter T cell line (GXR 25 cells) in 800 µl of R10 medium (RPMI 1640 medium containing 10% FCS, 2 mM L-glutamine, 100 U ml^{-1} penicillin and 100 µg ml^{-1} streptomycin) and transfected by electroporation using a Bio-Rad Gene Pulser II instrument (300 V and 500 uF). After transfection, cells were rested for 45 min at room temperature, transferred to T25 culture flasks in 5 ml of warm R10 and fed with 5 ml of R10 on day 4. GFP expression was monitored by flow cytometry (FACSCalibur, BD Biosciences), and, once GFP expression reached more than 30% among viable cells, supernatants containing the recombinant viruses were harvested and aliquots stored at −80 °C.

VRC assays

The replication capacity of each chimera was determined by infection of GXR cells at a low multiplicity of infection of 0.003, following the method of Miura et al.[65]. The mean slope of exponential growth from day 2 to day 7 was calculated using the semi-log method in Excel. This was divided by the slope of growth of the wild-type NL4-3 control included in each assay to generate a normalized measure of replication capacity. Replication assays were performed in triplicate, and results were averaged. These VRC determinations were undertaken entirely blinded to the identity of the study subject.

Single-genome amplification of viral RNA

For single-genome amplification of the gag-protease genes, RNA was endpoint diluted in 96-well plates such that fewer than 29 PCRs yielded an amplification product. According to a Poisson distribution, the cDNA dilution that yields PCR products in no more than 30% of wells contains one amplifiable cDNA template per positive PCR more than 80% of the time[80]. RT–PCR and second-round amplification were carried out as described above. PCR products were visualized by agarose gel electrophoresis under UV light using a Gel Doc 2000 (Bio-Rad). All products derived from cDNA dilutions yielding less than 30% PCR positivity were purified using a QIAquick PCR Purification Kit (Qiagen) and sequenced.

Viral RNA sequencing and phylogenetic analysis

Population sequencing was undertaken using the BigDye Ready Reaction Terminator Mix (V3) (Department of Zoology, University of Oxford) using *gag-protease* sequencing primers SQ2FC (CTT CAG ACA GGA ACA GAG GA), GF100-1817.18 (TAG AAG AAA TGA TGA CAG), gf2331 (GGA GCA GAT GAT ACA GTA TT), SQ16RC (CTT GTC TAG GGC TTC CTT GGT), GAS4R (GGT TCT CTC ATC TGG CCT GG), pan1dRx (CAA CAA GGT TTC TGT CAT CC), GR1981 (CCT TGC CAC AGT TGA AAC ATT T) and gr2536 (CAG CCA AGC TGA GTC AA). Sequence data were analyzed using Sequencher version 4.8 (Gene Codes Corporation). Nucleotides for each gene were aligned manually in Se-Al version 2.0a11. Maximum-likelihood phylogenetic trees were generated using PHYm131 (https://www.hiv.lanl.gov) and visualized using FigTree (http://tree.bio.ed.ac.uk/software/figtee/) version 1.2.2.

IFN-I sensitivity assays using the U87 MG/D1406 cell line

The U87 $CD4^+CCR5^+$ cells were obtained from the National Institutes of Health (NIH) HIV Reagent Program (cat. no. 4035), contributed by HongKui Deng and Dan Littman[81]. The U87/D1406 reporter cell line was generated by transduction with a lentivirus vector (K5534) comprising secreted nano-luciferase (snLuc), monomeric enhanced green fluorescence protein (EGFP) and puromycin (puro), wherein expression of these genes was placed under control of an HIV-1 long terminal repeat (LTR) (LTR-puro.T2A.EGFP-IRES-snLuc-LTR). The parental U87 $CD4^+CCR5^+$ cells are resistant to G418 and puro. Therefore, after transduction with the K5534 lentivector, the cells were FACS sorted to

isolate a population of cells exhibiting nominal GFP expression, thereby reducing the background level of snLuc expression from uninfected cells. The cells were further modified by transduction with a lentivirus vector (K5600) comprising the human CXCR4 co-receptor and the blasticidin resistance gene (BSD) that were placed under transcriptional control of the human EF1αpromoter (EF1α-CXCR4-IRES-BSD). The U87/D1406 reporter cells are sensitive to infection by either R5 or X4 strains of HIV-1. Infected cells express EGFP and snLuc that may be sampled directly from culture supernatants and analyzed to quantify HIV-1 infection and inhibition thereof.

To determine IFN-I concentrations required to inhibit virus replication to 50% (IC_{50}), U87-MG cells were left untreated or cultured in the presence of increasing amounts of IFN (0.0001 pg ml^{-1} to 1 pg ml^{-1}), infected with equal amounts of patient-specific gag-pro chimeric virus (multiplicity of infection 0.03) and cultured for 6 days (IFN-α-2α BioVision 4594-100 lot 6HO6L45940 and IFN-β BioVision 4860-50 lot 40460). IFN-containing medium was replenished every 24 h. Viral infectivity was measured using a luminescent reporter (Nano-Glo Luciferase Assay System, Promega) and quantified on a GloMax 96 microplate luminometer (Promega). Viral replication was plotted for each IFN concentration as the percentage of viral growth in the absence of IFN.

pVL

Plasma HIV-1 RNA viral load measurement for the Ucwaningo Lwabantwana cohort (2015–2023) was undertaken using the BioMérieux NucliSens Version 2.0 Easy Q/Easy Mag (NucliSens version 2.0) assay (dynamic range, 20–10 million HIV RNA copies per milliliter). Plasma HIV-1 RNA viral load measurement for the Paediatric Early HAART and Structured Treatment Interruption Study (PEHSS) cohort (2002–2005) was undertaken using the Roche Amplicor version 1.5 assay, with a lower limit of detection of 50 RNA copies per milliliter.

HIV-1 DNA analysis

Total HIV-1 DNA levels in the pediatric cohort were quantified using droplet-digital PCR (Bio-Rad) starting from 1×10^6 PBMCs. Samples were screened with three different primer/probe sets, two annealing to the 5′*LTR* and *gag* conserved regions of HIV-1 genome[82] and an additional *int-degenerated* primer/probe set adapted to clade C (iSCA-int Forward Degenerate TTTGGAAAGGACCAGCMAA, iSCA-int Reverse TGGAAAACAGATGGCAGG, iSCA-int Probe AAAGGTGAAGGGGCAGTAGTAATACA). Input cell number was verified by quantifying the amount of genomic *RRP30* gene, in a parallel droplet-digital PCR assay, and this value was used to infer the limit of detection for each sample. Viral DNA was further evaluated using PCR protocols designed to amplify near full-length, gag or pol clade C HIV-1 sequences, as described in Extended Data Table 3. Primers and reaction conditions for near full-length amplification were as described by Garcia-Broncano et al.[24], Lee et al.[25] and Dufour et al.[83]; for the latter experiments, the reverse primer of the second-round PCR was adapted to 5′-CTAGTTACCAGAGTCACACAACAGACG -3′. Primers and reaction conditions for amplification of gag were as described by Koofhethile et al.[26]; for the amplification of HIV-1 pol, the following primer pairs were used: forward primer 5′-GAAGGGCACATAGCCAGAAATTGCAGGG-3′, reverse primer 5′-GCTCCTGCTATGGGTTCTTTCTCCAGCTGG-3′; second-round nested PCR forward primer 5′-CCTAGGAAAAAAGGCTGTTGGAAATGTGG-3′, reverse primer 5′-CAAACTCCCACTCAGGAATCCA-3′.

Determination of plasma cART levels

We focused cross-sectionally on children enrolled in the first 30 months of the study ($n = 73$, median age 12 months, IQR 12–12 months) and, additionally, in longitudinal analyses, on the children aged ≥48 months in the cohort that had maintained aviremia consistently without any viral blips or spikes ($n = 25$). At baseline, all infants were initiated on AZT/3TC/NVP, which was switched at 1 month to ABC/3TC/LPV/RTV. We determined the levels of all 13 ART drugs prescribed in South Africa but focused on LPV because its plasma level is directly related to anti-viral activity; also, its half-life is longer than that of the nucleoside reverse transcriptase inhibitors, such as AZT, and, therefore, is less affected by variation in sampling time after dosing. Blood samples were taken in clinic within 2–4 h of the child being administered with cART, according to maternal history. Children were treated with the approved formulation of liquid. Plasma samples were analyzed using LC–MS/MS. The LC–MS/MS method for the simultaneous detection and quantitation of 13 anti-retroviral drugs was developed and validated according to US Food and Drug Administration guidelines for bioanalytical analysis[21,84]. The quantitative concentration range was 150–6,000 ng ml^{-1} for LPV. For values below 150 ng ml^{-1}, the concentration of drug can be determined with a degree of certainty if the signal-to-noise ratio for that particular sample is sufficiently high. Here, we used a signal-to-noise ratio of ≥3, as is widely accepted[85], for all values shown lower than 150 ng ml^{-1} but higher than 10 ng ml^{-1}. A 10× dilution using drug-free plasma was used to quantify drug levels in samples with drug levels above the upper limit of quantification. Sample analysis was performed using an Agilent 1200 series high-performance liquid chromatography (HPLC) system coupled to SCIEX QTRAP 5500 triple quadrupole mass spectrometer equipped with an electrospray ionization TurboIonSpray source. Calibration standards and quality control samples were prepared using drug-free, donor human plasma. The anti-retroviral drug analytes were extracted from standard, quality control and clinical samples using a protein precipitation method. The extracted analytes were chromatographically separated on an Agilent ZORBAX Eclipse Plus C18 (2.1 × 50 mm, 3.5 µm) HPLC column using gradient elution. The aqueous mobile phase A consisted of water with 0.1% formic acid, and mobile phase B consisted of acetonitrile with 0.1% formic acid. The HPLC column oven temperature was set at 40 °C; a sample volume of 2 µl was injected; and the flow rate was set to 0.2 ml min^{-1}. Mass spectrometry data acquisition was performed using polarity switching—for the simultaneous analyte ion selection and detection in positive and negative modes. Analysis was performed using multiple reaction monitoring at unit resolution, in positive scan mode, set to detect parent $[M + H]^+$ → product ion transitions for LPV; m/z 629.2 → m/z 120.6 and m/z 155.2. Data were collected and quantitated using Analyst software, version 1.6.2.

Statistical analysis

In scatter plots, median values and IQRs are indicated. Comparisons were performed using Fisher's exact test for categorical variables and Student's *t*-test or Mann–Whitney *U*-test for continuous variables. Maintenance of viral suppression was calculated using Kaplan–Meier analysis, and different groups were compared using the log-rank test. Univariate linear regression analyses were performed with $\log_{10}$ (MoM pVL) as response and either $\log_{10}$ (IFN-α IC_{50}) or $\log_{10}$ (IFN-β IC_{50}) as covariate, respectively. In addition, multivariate regression models were applied with $\log_{10}$ (child pVL) as the response and several covariates (DTG, age at enrollment (AaE), sex and the interaction between AaE and sex). All *P* values in these regression models were two-sided. All calculations and graphs were performed using R software[86] and GraphPad Prism version 7.

Reporting summary

Further information on research design is available in the Nature Portfolio Reporting Summary linked to this article.

Data availability

There are no restrictions on the availability of materials or information relating to this manuscript.

Code availability

The code is not available.

References

80. Björndal, A. et al. Coreceptor usage of primary human immunodeficiency virus type 1 isolates varies according to biological phenotype. *J. Virol.* **71**, 7478–7487 (1997).
81. Lorenzi, J. C. C. et al. Paired quantitative and qualitative assessment of the replication-competent HIV-1 reservoir and comparison with integrated proviral DNA. *Proc. Natl Acad. Sci. USA* **113**, E7908–E7916 (2016).
82. Moron-Lopez, S. et al. Sensitive quantification of the HIV-1 reservoir in gut-associated lymphoid tissue. *PLoS ONE* **12**, e0175899 (2017).
83. Dufour, C. et al. Phenotypic characterization of single CD4$^+$ T cells harboring genetically intact and inducible HIV genomes. *Nat. Commun.* **14**, 1115 (2023).
84. Food and Drug Administration Guidance for Industry. *Bioanalytical Method Validation* (US Department of Health and Human Services, Food and Drug Administration, Center for Drug Evaluation and Research, 2018); https://www.fda.gov/files/drugs/published/Bioanalytical-Method-Validation-Guidance-for-Industry.pdf
85. United Nations Office on Drugs and Crime. *Guidance for the Validation of Analytical Methodology and Calibration of Equipment Used for Testing of Illicit Drugs in Seized Materials and Biological Specimens* (United Nations, 2009); https://www.unodc.org/unodc/en/scientists/guidance-for-the-validation-of-analytical-methodology-and-calibration-of-equipment.html
86. R Core Team *R: A Language and Environment for Statistical Computing* (R Foundation for Statistical Computing, 2023).

Acknowledgements

This work received funding from the Wellcome Trust (PG WTIA Grant WT104748MA) and the National Institutes of Health (AI133673 and 1UO1AI168655-01 to P.G.; 1UM1AI164566 (the Pediatric Adolescent Virus Elimination (PAVE) Martin Delaney Collaboratory Grant) to P.G. and P.P.; AI184094, AI176579, AI155233 and AI152979 (all to M.L.); 1UM1AI164561-01 to J.M.-P.; UM1AI106716 and UM1AI068632 to E.C.; and eRA grant BX004547, VA Health Administration, Biomedical Laboratory R&D (to J.C.K.)). This study was also supported by the EPIICAL project (https://www.epiical.org) to N.C., P.P. and P.G., supported by PENTA-ID foundation (https://penta-id.org/) and funded through an independent grant by ViiV Healthcare UK. The funders played no role in either the design or execution of the study. We also would like to acknowledge the commitment of the dedicated study participants and clinicians, including P. Mbatha, J. Millar and M. Muenchhoff, to this work and to thank M. Altfeld, M. Malim and B. Walker for invaluable input and discussions.

Author contributions

N.B., G.C. and K.D. coordinated and managed cohort recruitment and maintenance and analyzed data. E.A., N.H., N.L. and K.R. performed experiments and analyzed data. R.F., K.S., V.V., S.K., J.v.L., K.C., C.K., R.B., M.K., J.R. and N.M. managed cohort recruitment and maintenance and analyzed data. G.R.P., N.C., P.P., A.T., P. Rojo, C.G. and P. Rossi performed experiments, analyzed data and contributed to writing of the manuscript. M.C.G.-G., C.O., S.H., M.C.P., M.L., J.M.-P. and J.C.K. performed experiments, analyzed data and helped write the manuscript. A.G., M.A.A. and E.C. analyzed data and helped write the manuscript. T.N. and M.A. co-supervised the project and contributed to data analyses and writing of the manuscript. P.G. conceived, designed and supervised the study, contributed to data analyses, obtained funding and wrote the manuscript.

Competing interests

The authors declare no competing interests.

Ethics and inclusion statement

Data for this study were collected in South Africa. Sixteen colleagues (N.B., G.C., N.H., R.F., K.G., K.S. S.K., J.v.L., K.C., C.K., R.B., M.K., N.M., K.R., T.N. and M.A.) are from South Africa, a low-and-middle-income country, including two of the three joint first authors (N.B. and G.C.). We fully endorse and are committed to the Nature Portfolio journals' guidance on low-and-middle-income country authorship and inclusion. This research is locally relevant to South Africa and other countries where HIV remains a major public health issue. The University of KwaZulu-Natal BREC (BF450/14) and the Oxfordshire Rec A Ethics Committee (06/Q1604/12) approved the study. The data collection and analysis techniques employed raised no risks pertaining to incrimination, discrimination, animal welfare, the environment, health, safety, security or other personal risks. All HIV testing was conducted at local laboratories. No cultural artifacts or associated traditional knowledge has been transferred out of any country. In preparing the manuscript, the authors reviewed relevant studies from South Africa.

Additional information

Extended data is available for this paper at https://doi.org/10.1038/s41591-024-03105-4.

Supplementary information The online version contains supplementary material available at https://doi.org/10.1038/s41591-024-03105-4.

Correspondence and requests for materials should be addressed to Philip Goulder.

Peer review information *Nature Medicine* thanks Ria Goswami and the other, anonymous, reviewer(s) for their contribution to the peer review of this work. Primary Handling Editor: Alison Farrell, in collaboration with the *Nature Medicine* team.

https://doi.org/10.1038/s41591-024-03105-4

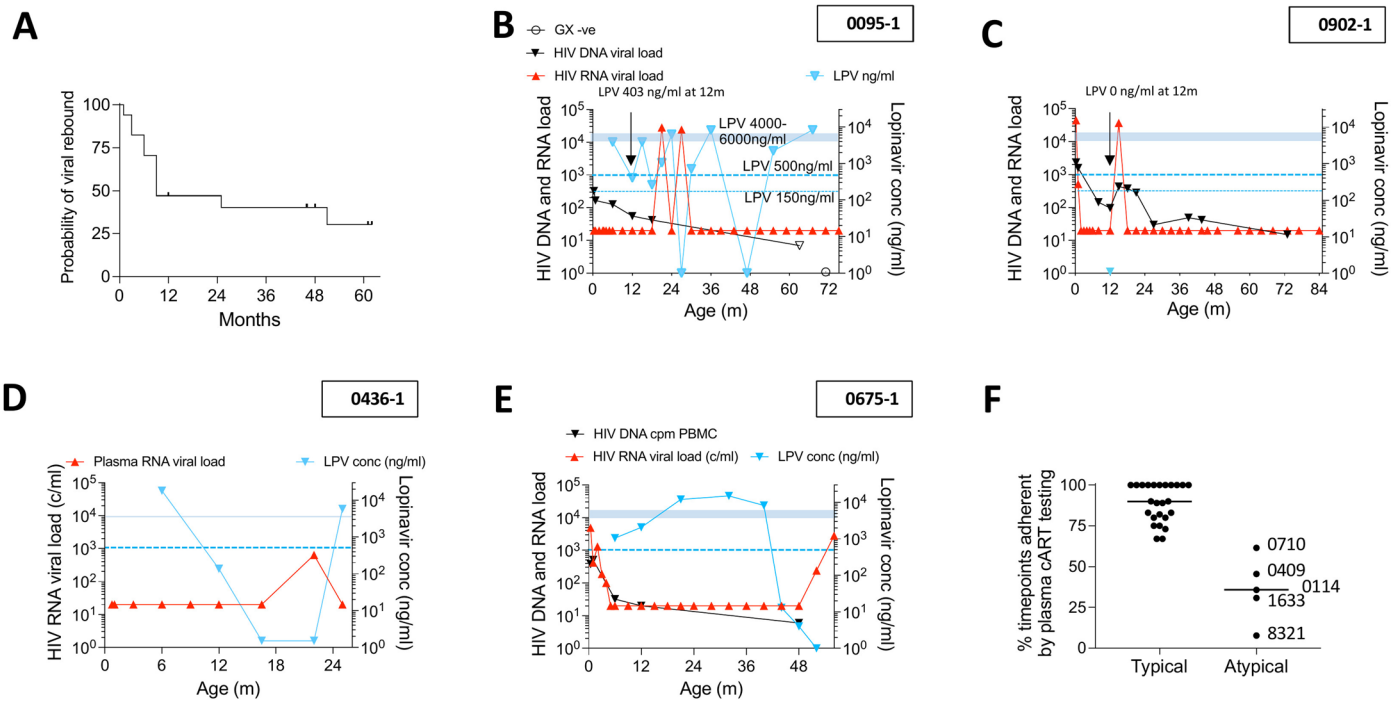

Extended Data Fig. 1 | cART non-adherence in children identified by plasma cART testing. a. Time to viral rebound in children aviraemic but with low LPV levels at 12m (in Fig. 2a). **b-c**. Two examples of viral rebound following low levels of LPV detected at 12m (in Fig. 2a). **d-e**. Two examples of children followed longitudinally illustrating viral rebound following detection of low cART levels at later timepoints in the plasma. **f**. Proportion of timepoints when lopinavir levels were low in 25 'typical' children maintaining aviraemia to age ≥48m without blips or spikes compared with the 5 'atypical' children.

https://doi.org/10.1038/s41591-024-03105-4

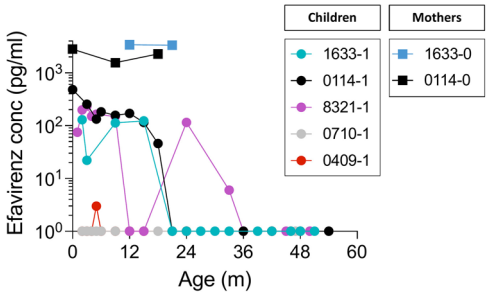

Extended Data Fig. 2 | Plasma Efavirenz levels in the 5 'atypical' children and in two of their mothers. The mothers 1633-0 and 0114-0 have the subscript -0, the children have the subscript -1. Three children were breast-fed, 60-1633-1, 80-0114-1 and 60-8321-1; two children, 70-0710-1 and 80-0409-1, were not breast-fed.

https://doi.org/10.1038/s41591-024-03105-4

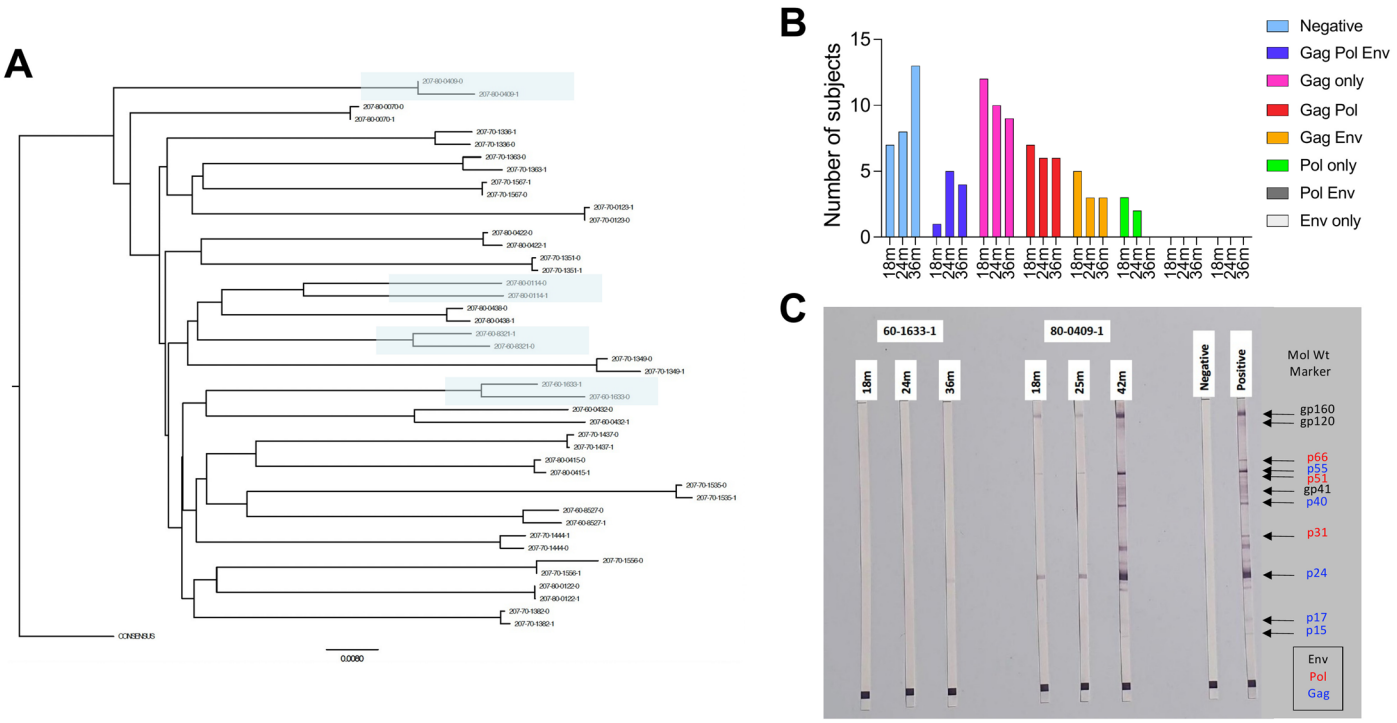

Extended Data Fig. 3 | Phylogenetic clustering of mother-child pair *gag* sequences and Western blot testing of plasma samples at 18m, 24m and 36m from children within the study cohort. a. A maximum likelihood tree constructed using full-length *gag* sequences shows mother-child clustering of sequences for 22 representative mother-child pairs within the cohort, including 4 of the 'atypical' pairs 60-1633-0/1, 80-0114-0/1, 60-8321-0/1, and 80-0409-0/1 (shaded). Maternal sequences carry the suffix -0 and child sequences carry the suffix -1. **b**. Western blot reactivities for 35 children who maintained plasma viral loads at <20c/ml at all timepoints to 36m following suppression. These data include the 3 'atypical' children, 60-1633-1, 80-0114-1 and 70-0710-1, who maintained plasma viral loads at <20c/ml at all timepoints to 36m following suppression. **c**. Western blot results for two of the 'atypical' children, 60-1633-1 and 80-0409-1 at the timepoints shown. These data are representative of experiments run in triplicate.

https://doi.org/10.1038/s41591-024-03105-4

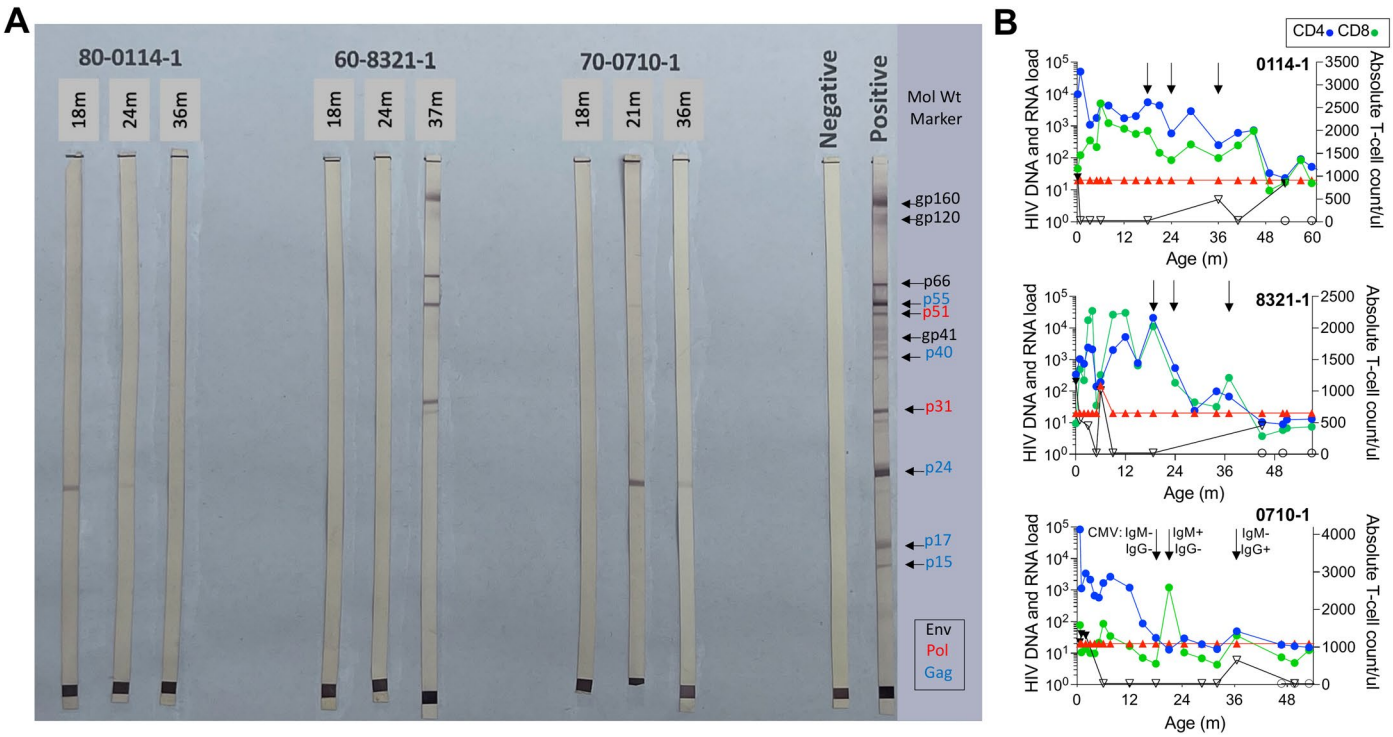

Extended Data Fig. 4 | Evidence of HIV infection in the 'atypical' male participants from Western Blot testing. a-b. Transient anti-HIV antibody detection at age ≥18m in plasma samples from the 3 'atypical' children whose baseline plasma HIV RNA viral loads were undetectable. These data are representative of experiments run in triplicate. **a.** Western blot testing of plasma samples from 70-0710-1, 60-8321-1 and 80-0114-1 at 18m-36m timepoints. **b.** Plasma HIV RNA viral loads, HIV DNA loads, absolute CD4 count and absolute CD8 count in participants 80-0114-1, 60-8321-1 and 70-0710-1. Symbols as in Fig. 2; blue circles: absolute CD4 counts; green circles: absolute CD8 counts. Arrows show timepoints used for Western blot assays. In 70-0710-1, CMV-specific IgM was undetectable at 18m and 36m and was detectable at 21m; CMV-specific IgG was undetectable at 18m and 21m but detectable at 36m.

https://doi.org/10.1038/s41591-024-03105-4

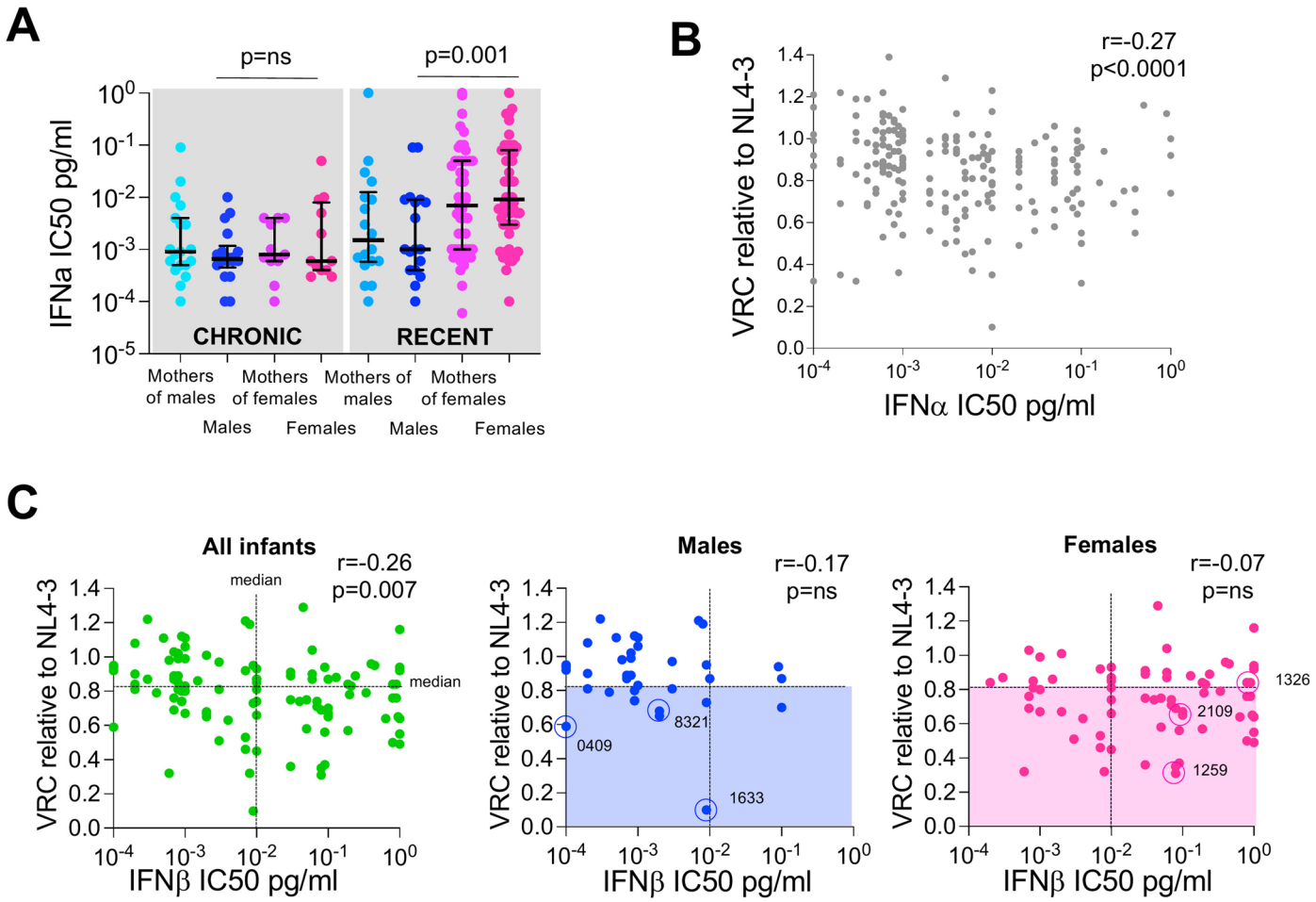

Extended Data Fig. 5 | Inverse correlation between VRC and IFN-I resistance in study cohort. a. IFNa IC50 values determined for 98 mother-child pairs in the cohort. P values were determined using the two-tailed Mann-Whitney U test. **b**. Inverse correlation overall in study cohort between VRC and IFNa IC50. Data are presented as median and interquartile range. The P value was determined using the two-tailed Student's *t*-test. **c**. Relationship between VRC and IFNa IC50 in viruses transmitted to males and to females. Blue open circles highlight males maintaining aviraemia despite cART non-adherence. In the case of 80-0114-1, viral replication was detectable but at levels too low to measure VRC; therefore IFN-I IC50 could not be determined for this child. Red open circles highlight viruses transmitted to the female twin but not to the male twin within 3 of 5 sex-discordant twinsets evaluated where, in each case, transmission only occurred in the female twin. Blue shading highlights viruses transmitted to males below the median VRC for all infants; red sharing highlights viruses transmitted to females below the median VRC for all infants. r values represent Spearman's rank correlation coefficient. The P values were determined using the two-tailed Student's *t*-test.

https://doi.org/10.1038/s41591-024-03105-4

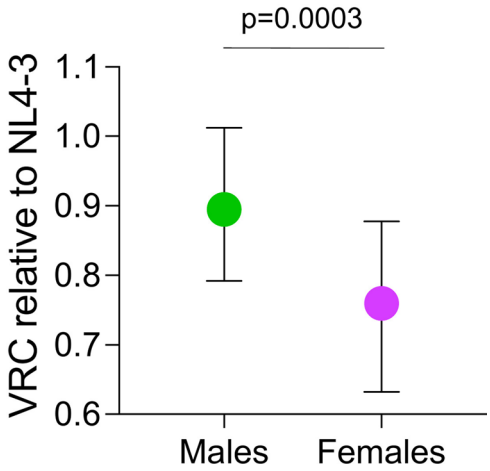

Extended Data Fig. 6 | Baseline viral replicative capacities in male and female infants. Males n = 36, females n = 68. Data are presented as median and interquartile range. P value determined using the two-sided Mann-Whitney U test.

https://doi.org/10.1038/s41591-024-03105-4

Extended Data Table 1 | A multivariate regression model to determine the impact on child pVL at baseline of the DTG era, child AaE (days), sex of child and the interaction between sex of child and AeE

	β coefficient	p value
Reference*	3.89	n/a
Pre-DTG	+0.54	0.006
Male sex	-0.70	0.01
Age at enrolment (d)	-0.06	0.002
Interaction: Male/Age at Enrolment	0.05	0.04

*Reference: Child $\log_{10}$ pVL for:
DTG era, Female sex, Enrolment at 0d

The model was applied with $\log_{10}$ (child pVL) as the response and DTG, AaE, sex of child and the interaction between AaE and sex of child as the covariates. All *P* values in this regression model were determined using two-sided Student's *t*-tests.

https://doi.org/10.1038/s41591-024-03105-4

Extended Data Table 2 | Summary of relevant clinical features of the atypical group of five children compared to the 'typical' group of age-matched children

	60-1633-1	80-0114-1	60-8321-1	70-0710-1	80-0409-1	'Atypical' Group n=5	'Typical' Group n=25
Age (m): median (IQR) [a]	86	69	59	64	59	64 (59-78)	65 (57-76)
Non-adherence by hx [b]	4 x 5-13wk	1 x 7m	1 x 8m	2 x 2.5-10m	[Poor adherence]	4/5	0/25
Low plasma cART [c]	9/13	9/14	12/13	5/13	5/11	42/65 (65%)	31/207 (15%)
Clinic non-attendance [d]	Lftu x 2: 9-10m	Missed no clinics	Ltfu x 8m	Ltfu x 10m	Ltfu x 17m	4/5	0/25
HIV DNA load <LoD [e]	0m	1m	1m	6m	1m	5/5 by 12m	7/24 by 12m
Mat. seroconversion [f]	19-38wk gest.	26-37wk gest.	10m pre-preg. to 21wk gest.	3yrs pre-preg.	14yrs pre-preg.		
Maternal cART [g]	FTC/TDF/EFZ	FTC/TDF/EFZ	FTC/TDF/EFZ	FTC/TDF/EFZ	FTC/TDF/EFZ		
Maternal pVL (c/ml) [h]	Seroconverter	Seroconverter	107,000 at 21wk	180 (delivery)	50,000 (delivery)		
Gestation at delivery	38wks	38wks	38wks	40wks	38wks		
Duration breast-fed [i]	18m	24m	18m	Not breast-fed	Not breast-fed		
Infant ART prophylaxis	NVP	AZT/NVP	AZT/NVP	AZT/NVP	NVP		
Age at cART initiation	d1	d7	d1	d20	d14		
Child HLA-I type	A*01:01/68:02 B*15:10/81:01 C*03:04/18:01	A*29:02/43:01 B*15:03/42:01 C*17:01/18:01	A*03:01/66:01 B*58:02/58:02 C*06:02/06:02	A*23:01/30:02 B*14:02/44:03 C*02:02/08:02	A*74:01/74:01 B*15:03/57:03 C*02:02/07:01		
Maternal HLA-I type	A*01:01/66:01 B*58:01/81:01 C*07:01/18:01	A*03:01/43:01 B*13:02/15:03 C*06:02/18:01	A*26:01/66:01 B*39:10/58:02 C*06:02/12:03	A*02:01/23:01 B*44:03/58:01 C*02:02/03:02	A*74:01/74:01 B*15:03/35:01 C*02:02/04:01		

[a] Ages at 07/2023. [b] cART discontinuation by history from the mother. [c] Timepoints with low plasma cART levels. [d] Ltfu: loss to follow up.
[e] Age at which total HIV DNA load was first undetectable (either 0 copies/million pbmc or not significantly different from 0 copies/million pbmc).
[f] 60-8321-0 (mother) tested HIV antibody negative 10m prior to the pregnancy and antibody positive at 21wks gestation.
[g] Maternal cART regimens ante-natally and post-natally did not alter during the breast-feeding period. [h] 60-1633-0 and 80-0114-0 (mothers) both tested HIV antibody negative in pregnancy prior to a positive test at delivery and at 37wks gestation, respectively. [i] by history from the mother

https://doi.org/10.1038/s41591-024-03105-4

Extended Data Table 3 | Summary of PCR reactions for analyzing HIV-1 DNA by single-genome amplification

Participant ID	Clade C gag PCR (Koofhethile et al.[34])	Clade C pol PCR (internal lab primers)	Clade C nFL PCR (forward primers per Koofhethile et al.[34], reverse primers per Lee et al.[33])	Clade C nFL PCR (Dufour et al.[81])	Clade C nFL PCR (Lee et al.[33], Garcia-Broncano et al.[32])	Sum
207-60-8321	481,000	251,000	302,000	481,000	9,830,000	11,345,000
207-70-0710	356,000	256,000	356,000	1,070,000	4,400,000	6,438,000
207-80-0409	335,000	249,000	605,000	1,210,000	5,680,000	8,079,000
207-80-0114	330,000	248,000	712,000	1,100,000	9,760,000	12,150,000
207-60-1633	340,000	251,000	673,000	1,130,000	7,070,000	9,464,000

Numbers of PBMCs subjected to each type of PCR reaction are indicated. nFL, near full-length.

https://doi.org/10.1038/s41591-024-03105-4

Extended Data Table 4 | Tests undertaken that determined HIV infection status in the five 'atypical' children maintaining aviremia despite cART non-adherence

	60-1633-1	80-0114-1	60-8321-1	70-0710-1	80-0409-1
Dried blood spot Qualitative TNA PCR	Indeterminate	Positive (d0)	-ve (d1)	Positive (d0)	Positive (d0)
Whole blood Qualitative DNA PCR	Not done	Positive (d7)	-ve (d1)	Positive (d30)	Positive (d14)
Whole blood TNA PCR GX (Cepheid)	Positive (d0)	Not done	Positive (d1)	Positive (d20)	Not done
Plasma HIV RNA Viraemia (c/ml)	1100 (d0)	<20c/ml	150 (6m)	<20c/ml	24,000 (d14) 430 (15m)
Total HIV DNA (ddPCR; cpm pbmc)	19 (6m) 21 (18m)	25 (d7)	199 (d1) 104 (6m)	22 (d20) 36-40 (1-2m)	5 (d14) 85 (15m)
Phylogenetic clustering of MC pair *gag* sequence	Positive (d0)	Positive (d7)	Positive (d1)	*gag* not amplified	Positive (d14)
Western blots (18m/24m/36m)	neg/neg/ind	ind/ind/neg	neg/neg/ind	neg/ind/ind	ind/ind/pos

nature portfolio

Corresponding author(s): PROFESSOR PHILIP GOULDER

Last updated by author(s): May 22, 2024

Reporting Summary

Nature Portfolio wishes to improve the reproducibility of the work that we publish. This form provides structure for consistency and transparency in reporting. For further information on Nature Portfolio policies, see our Editorial Policies and the Editorial Policy Checklist.

Statistics

For all statistical analyses, confirm that the following items are present in the figure legend, table legend, main text, or Methods section.

n/a	Confirmed	
☐	☒	The exact sample size (*n*) for each experimental group/condition, given as a discrete number and unit of measurement
☐	☒	A statement on whether measurements were taken from distinct samples or whether the same sample was measured repeatedly
☐	☒	The statistical test(s) used AND whether they are one- or two-sided *Only common tests should be described solely by name; describe more complex techniques in the Methods section.*
☐	☒	A description of all covariates tested
☐	☒	A description of any assumptions or corrections, such as tests of normality and adjustment for multiple comparisons
☐	☒	A full description of the statistical parameters including central tendency (e.g. means) or other basic estimates (e.g. regression coefficient) AND variation (e.g. standard deviation) or associated estimates of uncertainty (e.g. confidence intervals)
☒	☐	For null hypothesis testing, the test statistic (e.g. *F*, *t*, *r*) with confidence intervals, effect sizes, degrees of freedom and *P* value noted *Give P values as exact values whenever suitable.*
☒	☐	For Bayesian analysis, information on the choice of priors and Markov chain Monte Carlo settings
☒	☐	For hierarchical and complex designs, identification of the appropriate level for tests and full reporting of outcomes
☐	☒	Estimates of effect sizes (e.g. Cohen's *d*, Pearson's *r*), indicating how they were calculated

Our web collection on statistics for biologists contains articles on many of the points above.

Software and code

Policy information about availability of computer code

Data collection	Excel for Mac v16.3, DataFax v 2016.0.0 and DF Discover version 5.1.0 were used to collect data from the Ucwaningo Lwabantwana study
Data analysis	GraphPad Prism version 7.0b R code (89. R Core Team R: A Language and Environment for Statistical Computing. R Foundation for Statistical Computing, Vienna, Austria. URL: https://www.R-project.org/. (2023). and FlowJo version 10.8.2

For manuscripts utilizing custom algorithms or software that are central to the research but not yet described in published literature, software must be made available to editors and reviewers. We strongly encourage code deposition in a community repository (e.g. GitHub). See the Nature Portfolio guidelines for submitting code & software for further information.

Data

Policy information about availability of data

All manuscripts must include a data availability statement. This statement should provide the following information, where applicable:

- Accession codes, unique identifiers, or web links for publicly available datasets
- A description of any restrictions on data availability
- For clinical datasets or third party data, please ensure that the statement adheres to our policy

There are no restrictions on the availability of materials or information relating to this manuscript. The data that support the findings in this study are available from the corresponding authors upon reasonable request.

Human research participants

Policy information about studies involving human research participants and Sex and Gender in Research.

Reporting on sex and gender	169 of the infants enrolled were females and 115 were males.
Population characteristics	The Ucwaningo Lwabantwana is a cohort of 284 in utero-infected children enrolled and followed in KwaZulu-Natal, South Africa from 2015-2023. At enrolment, the median age of the infants was 8d, and the median absolute CD4 count, CD4% and plasma viral load were 1987 copies/ul, 43.5% and 4250c/ml, respectively. At enrolment, the median age of the mothers was 25yrs, and the median absolute CD4 count, CD4% and plasma viral load were 475 copies/ul, 24% and 3400c/ml, respectively. The median age of the children enrolled at date 07/31/2023 was 4yrs 10m.
Recruitment	This has been described in detail in the text in the section entitled "Study subjects". All babies born to HIV positive mothers were tested at birth and if HIV positive were recruited for study. There was no selection bias in the recruitment process.
Ethics oversight	The Biomedical Ethics Research Committee, University of KwaZulu-Natal and the Oxford Research Ethics Committee approved the studies.

Note that full information on the approval of the study protocol must also be provided in the manuscript.

Field-specific reporting

Please select the one below that is the best fit for your research. If you are not sure, read the appropriate sections before making your selection.

☒ Life sciences ☐ Behavioural & social sciences ☐ Ecological, evolutionary & environmental sciences

For a reference copy of the document with all sections, see nature.com/documents/nr-reporting-summary-flat.pdf

Life sciences study design

All studies must disclose on these points even when the disclosure is negative.

Sample size	Sample sizes were determined by considerations of sample availability, study resources, and previous paediatric cohort studies we have undertaken in South Africa (eg Muenchhoff et al Sci Transl Med 2016) where the numbers studied had allowed statistically significant immune predictors of disease outcomes to be made. No statistical methods were used to predetermine sample sizes.
Data exclusions	No data were excluded from analyses
Replication	Determination of viral replication capacities, interferon-resistance IC50, ddPCR determinations of HIV DNA load are all highly reproducible and are assays with a high degree of precision. In the case of the VRC and ddPCR assays these are performed in triplicate. All attempts at replication were successful. In each case the reproducibility of the data from these assays has been demonstrated by repeat testing on a subset of the samples.
Randomization	All mothers and infants were from the same ethnic population (South Africa).
Blinding	All the analyses were done blinded to sex of the subject.

Reporting for specific materials, systems and methods

We require information from authors about some types of materials, experimental systems and methods used in many studies. Here, indicate whether each material, system or method listed is relevant to your study. If you are not sure if a list item applies to your research, read the appropriate section before selecting a response.

Materials & experimental systems

n/a	Involved in the study
☒	☐ Antibodies
☐	☒ Eukaryotic cell lines
☒	☐ Palaeontology and archaeology
☒	☐ Animals and other organisms
☒	☐ Clinical data
☒	☐ Dual use research of concern

Methods

n/a	Involved in the study
☒	☐ ChIP-seq
☐	☒ Flow cytometry
☒	☐ MRI-based neuroimaging

Eukaryotic cell lines

Policy information about cell lines and Sex and Gender in Research

Cell line source(s)	CEM-GXR cells were provided by collaborators Mark Brockman at Simon Fraser University, Canada. U87 MG/D1406 cell line were provided by collaborators John Kappes at University of Alabama at Birmingham, Birmingham, Alabama, USA. These cell lines are not commercially available.
Authentication	CD4 and CXCR4 expression on CEM-GXR and U87 cells were verified in-house by flow cytometry; and NL4-3 used as a positive control to assess cell permissiveness to virus infection.
Mycoplasma contamination	These cell lines were received mycoplasma, bacteria and fungi free; a new vial of cells was received and used. No in-house testing for mycoplasma contamination was done in addition.
Commonly misidentified lines (See ICLAC register)	No commonly misidentified cell line was used in this study.

Flow Cytometry

Plots

Confirm that:

☐ The axis labels state the marker and fluorochrome used (e.g. CD4-FITC).

☐ The axis scales are clearly visible. Include numbers along axes only for bottom left plot of group (a 'group' is an analysis of identical markers).

☐ All plots are contour plots with outliers or pseudocolor plots.

☐ A numerical value for number of cells or percentage (with statistics) is provided.

Methodology

Sample preparation	CEM-GXR cells were harvested daily, fixed in 2% PFA and acquired on the flow cytometer for quantification of GFP expression.
Instrument	BD LSR II
Software	FlowJo Software (Tree Star Inc., Ashland, OR).
Cell population abundance	GFP expression was quantified using CEM-GXR cell lines, no post-sorting of cells was involved.
Gating strategy	Live cells were identified based on SSC-A FSC-A distribution. FITC-A channel was utilized to quantify GFP expression. GFP+ populations were determined using an uninfected population of CEM-GXR as a negative control. No gating strategy was adopted here as a single population of GXR cells was used.

☐ Tick this box to confirm that a figure exemplifying the gating strategy is provided in the Supplementary Information.